139. Catalytic Cyclophanes

Part VIII[1])

Cytochrome P-450 Activity of a Porphyrin-Bridged Cyclophane

by David R. Benson[a]), Robert Valentekovich[a]), Suk-Wah Tam[a]), and François Diederich[b])*

a) Department of Chemistry and Biochemistry, University of California at Los Angeles,
Los Angeles, California 90024-1569, USA
b) Laboratorium für Organische Chemie, ETH-Zentrum, Universitätstrasse 16, CH–8092 Zürich

(15.IV.93)

Following a known synthetic procedure, the porphyrin-cyclophane **1** having a porphyrin attached by two straps to an apolar cyclophane binding site was prepared. Upon metallation, the Zn^{II} and Fe^{III} derivatives **2** and **3**, respectively, were obtained in good yields. Treatment of **3** with base yielded the μ-oxo dimer **4** in which the two oxo-bridged porphyrins moieties are both capped by cyclophane binding sites. All compounds **1**–**4** are freely soluble in protic solvents such as MeOH and CF_3CH_2OH, and the Fe^{III} derivatives **3** and **4** are active cytochrome P-450 mimics in these protic environments. Strong inclusion complexation of polycyclic aromatic hydrocarbons by **1** and **3** in alcoholic solvents was observed and quantified by ^1H-NMR and UV/VIS titrations. Acenaphthylene binds in an 'equatorial' orientation which locates its reactive 1,2-double bond near the porphyrin center, whereas phenanthrene binds 'axially' with the reactive 9,10-double bond oriented away from the porphyrin. The reduction potential of **3** was not significantly altered by substrate binding. In the unbound form, the Fe^{III} center in porphyrin **3** was found by ESR and ^1H-NMR to prefer a high-spin state ($S = 5/2$). In CF_3CH_2OH, using iodosylbenzene as O-transfer agent, the Fe^{III} derivative **3** catalyzed the oxidation of acenaphthylene to acenaphthen-1-one (**14**). Phenanthrene inhibited the reaction, possibly as a result of strong but nonproductive binding. Under similar conditions, isotetralin (**18**) was aromatized with high turnover to 1,4-dihydronaphthalene. The μ-oxo dimer **4** also showed high catalytic activity in the oxidation of acenaphthylene in MeOH, a result which provides strong evidence for efficient supramolecular catalysis. Due to as yet unknown reaction channels leading to polymeric products, poor mass balances were generally obtained in the oxidations effected in MeOH and CF_3CH_2OH in the presence of PhIO.

1. Introduction. – In efforts to model the properties of heme-containing enzymes, chemists have prepared a multitude of superstructured porphyrins [2]. Capped, bridged, or strapped porphyrins mimic *i*) the oxygen-transport and -storage proteins hemoglobin and myoglobin [3], *ii*) the oxygen-reducing cytochrome C oxidase [4], *iii*) the heme chromophores involved in the primary electron transfer processes at photosynthetic reaction centers [5], and *iv*) the hydrocarbon-oxidizing cytochrome P-450 enzymes [6].

Cytochrome P-450 enzymes are ubiquitous in nature and represent a versatile class of biological oxidation catalysts in both animals and in bacteria [7]. In their function as monooxygenases, they catalyze the transfer of one atom from dioxygen to their substrates while the other is split off as water (*Eqn. 1*). Some mammalian P-450 cytochromes are involved in the biosynthesis and degradation of endogenous steroids and lipids, while others have exogenous lipophilic drugs and environmental toxins as substrates. While the

---

[1]) Part VII: [1].

genes for some P-450 isozymes are continually active, the expression of others, particularly those whose substrates are exogenous, is induced only by the presence of the proper substrate [8]. Reactions catalyzed by the P-450 enzymes include N-, O-, and S-dealkylations, formation of heteroatom oxides such as sulfoxides, nitrogen and phosphine oxides, and even C–C bond cleavage in the biosynthesis of some steroidal hormones. Tremendous interest of the synthetic-chemistry community in cytochrome P-450 enzymes arises primarily as a result of their ability to selectively oxidize unactivated hydrocarbons. These reactions include hydroxylation of aromatic compounds and alkanes and epoxidation of alkenes and polycyclic aromatic hydrocarbons. H_2O-Solubility provided by oxidation of exogenous lipophilic substances represents the predominant mechanism for enzymatic detoxification of these materials in humans. However, with some polycyclic aromatic hydrocarbons such as benzo[a]pyrene, the same transformation can result in the formation of powerful carcinogens [9].

$$R + O_2 + 2\,H^+ + 2\,e^- \rightarrow R - O + H_2O \tag{1}$$
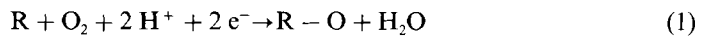
A large body of biochemical studies [7] and X-ray structural data [10] have provided significant insight into the structure and mode of action of the P-450 cytochromes. For monooxygenase activity, molecular O_2 is bound by the heme Fe^{II} (*Scheme 1*). In a sequence of redox processes, the bound O_2 is cleaved with formation of H_2O and a high-valent oxo-iron complex believed to be [$Fe^{IV}(=O)(porph^+)$]. This highly unstable oxo-iron complex, which was never directly observed in the enzyme, subsequently transfers its O-atom to the complexed substrate. Two structural features are characteristic for these enzymes: *1*) An iron porphyrinate forms one side of the O- and substrate-binding site. This site, deeply buried in the protein, is comprised almost entirely of hydrophobic amino-acid residues and, therefore, is of pronounced hydrophobic character. The polarity of the binding site both provides a driving force for the complexation of lipophilic substrates and modulates the reduction potential of the heme [11]. No additional catalytically active groups can be found at this hydrophobic site. *2*) A cysteinyl ligand, located on the porphyrin side opposite to the substrate-binding site, acts as an axial ligand of the heme-bound Fe-atom and is believed to provide a push to promote cleavage of the O–O bond in step *c*) of *Scheme 1* [12].

Scheme 1. *Catalytic Cycle of Cytochrome P-450 Monooxygenases and P-450 Enzyme Mimics* (S = substrate)
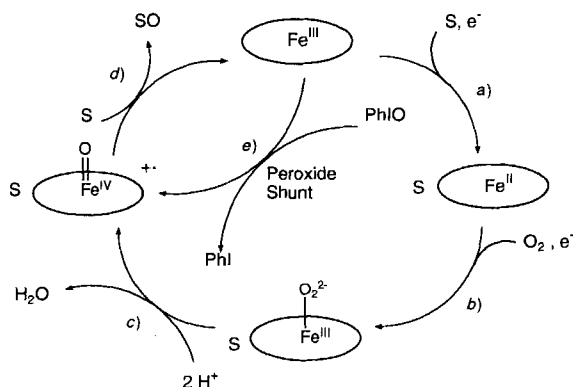
Over the past decade, chemists have become very interested in exploring the mechanism and synthetic potential of olefin epoxidations and alkane hydroxylations catalyzed by simple cytochrome P-450 model systems [13]. High catalytic turnovers and remarkable regio- and stereoselectivities [14] were reported for these reactions. In the majority of these studies, the natural process of oxygen activation was circumvented, and the catalytically active oxo-iron intermediate was generated by direct reaction of iron(III) porphyrinates with oxygen-transfer agents such as iodosylbenzene [15]. In contrast, the hydroxylation of aromatic hydrocarbons received only limited attention, mainly due to the low reactivity towards aromatic nuclei exhibited by most P-450 model compounds [16]. After having previously prepared a variety of efficient apolar cyclophane receptors for aromatic substrates [17], we became interested in constructing a cytochrome P-450 mimic which contains such a receptor in close proximity to an iron heme and would both bind and oxidize polycyclic aromatic hydrocarbons [18]. Although a number of porphyrin receptors were prepared [19], systems for the selective complexation of polycyclic aromatic hydrocarbons in protic solvents were not known at the start of this study. Investiga-

1	M = 2 H	X = EtN
2	M = Zn	X = EtN
3	M = Fe-Br	X = EtHN⁺ Br⁻
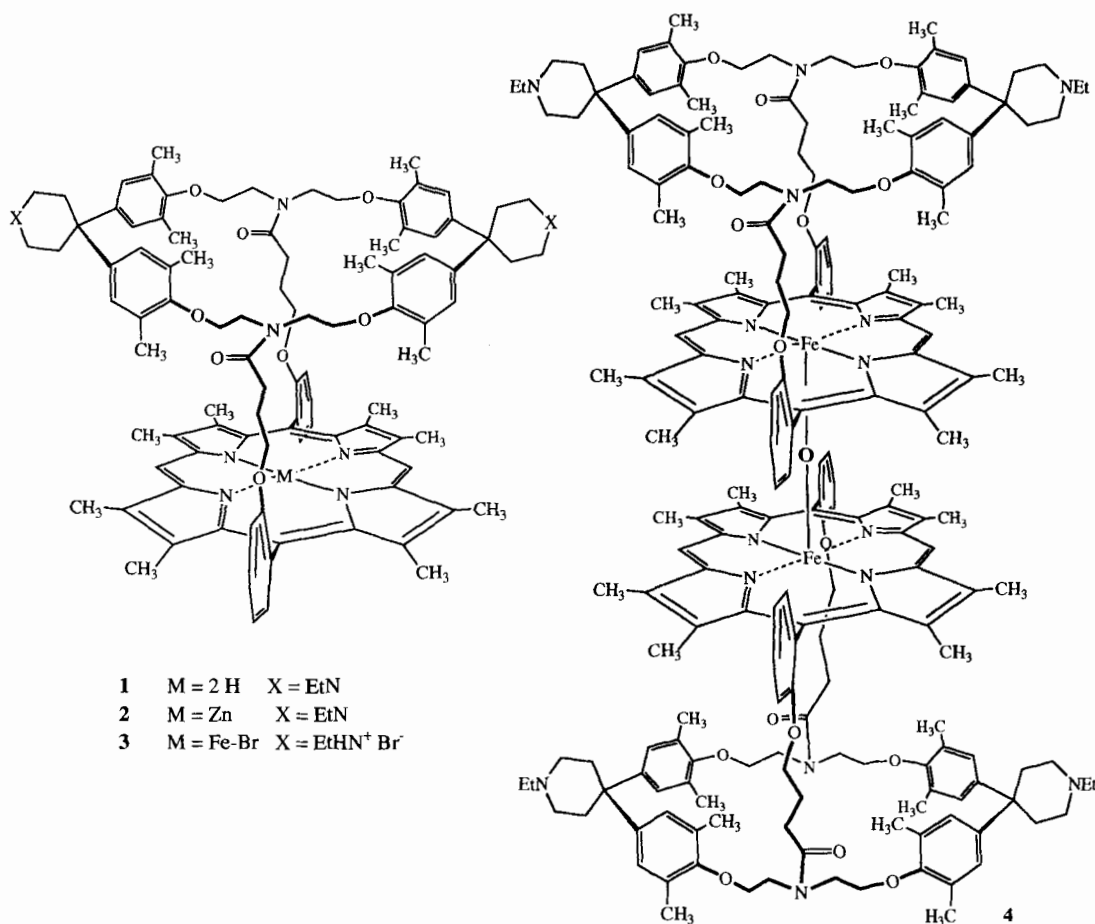
tions with such an artificial enzyme could provide valuable insights into the catalytic mechanisms for arene hydroxylation that are utilized by the natural systems. An additional interest to the projected studies came from the perspective of developing new homogeneous catalysts for synthetically useful arene hydroxylations. In this paper, we describe the synthesis of the porphyrin-cyclophane **3** and the corresponding μ-oxo dimer **4** and investigations of the complexation and catalytic properties of these novel cytochrome P-450 mimics.

2. Results and Discussion. – 2.1. *Synthesis of the Porphyrin-cyclophanes* **1–4**. The synthesis of porphyrin-cyclophane **1** follows a protocol previously developed by *Baldwin* and coworkers for the construction of strapped porphyrins as models for the oxygen-transport and -storage enzymes [20] (see *Scheme 2*). For the preparation of the starting

Scheme 2. *Synthesis of Porphyrin-cyclophane* **1**
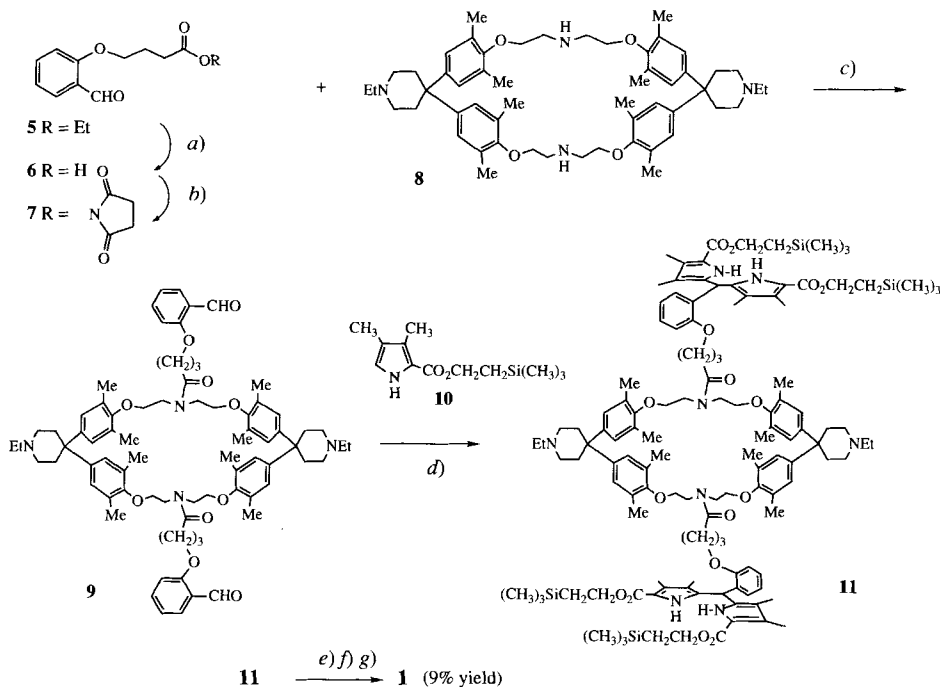
a) 2N KOH, MeOH, 85%. b) DCC, N-hydroxysuccinimide, THF, 87%. c) 1,4-Dioxane, 80°, 2 h, 75%. d) 2.1 equiv. of MeSO$_3$H, EtOH, reflux, 75%. e) Bu$_4$NF, THF, 50°, 2 h. f) CH(OMe)$_3$, CCl$_3$COOH, Zn(OAc)$_2$·2 H$_2$O, CH$_2$Cl$_2$. g) Conc. HCl, MeOH.

activated ester **7**, salicylaldehyde was reacted in a *Williamson* ether synthesis with ethyl 4-bromobutyrate (DMF, K$_2$CO$_3$, 70°) to give ester **5** in 93% yield. After saponification with 2N KOH in refluxing MeOH (→**6**, 85% yield) coupling with N-hydroxysuccinimide in tetrahydrofuran (THF) in the presence of dicyclohexylcarbodiimide (DCC) yielded **7** (87%).

The dialdehyde **9** was prepared in 75% yield by heating the previously reported cyclophane tetraamine **8** [21a] with 2.2 equiv. of **7** in refluxing 1,4-dioxane, followed by chromatography on silica gel (*Scheme 2*). For the condensation to the macrocyclic bis(dipyrromethane) **11**, 2-(trimethylsilyl)ethyl 3,4-dimethyl-1*H*-pyrrole-2-carboxylate (**10**) was synthesized in 78% yield by heating a solution of ethyl 3,4-dimethyl-1*H*-pyrrole-2-carboxylate [22] in 2-(trimethylsilyl)ethanol under vacuum at 90–100° with a catalytic amount of NaOMe. Condensation of **9** with four equiv. of **10** in the presence of catalytic amounts of MeSO₃H gave the protected bis(dipyrromethane)-cyclophane **11** in 75% yield.

Under the *Baldwin* protocol, the immediate precursor to the porphyrin **2** is the bis(dipyrromethane) obtained by deprotection of the 2-(trimethylsilyl)ethyl ester **11** and subsequent acid-catalyzed decarboxylation. Deprotection of ester **11** was effected with Bu₄NF in dry THF at 45–50° [23] (TLC monitoring (reversed-phase, MeOH/H₂O 9:1): spots for **11**, product, and all three partially deprotected intermediates). The reaction was complete within 2 h, and the crude tetracarboxylic acid isolated as an orange-yellow foam after removal of the solvent (¹H-NMR: complete disappearance of the resonance at 4.28 ppm (OCH_2CH₂SiMe₃), CH(pyr)₂ signal at 5.87 ppm unchanged). The zinc porphyrinate **2** was prepared by reaction of the crude tetracarboxylate with trimethyl orthoformate, CCl₃COOH, and Zn(OAc)₂ · 2 H₂O in CH₂Cl₂ for 44 h at 20°. Two atropisomers were formed, interconvertible by rotation about the bond between the porphyrin and the *meso*-aryl group. They were separated by flash chromatography (FC; silica gel, AcOEt/Et₃N 95:5) giving the major isomer (*R*_f 0.30) in 9% yield. Based on its ¹H-NMR spectrum (see below, *Fig. 1*), it was assigned structure **2** with an open preorganized binding site. The minor isomer (*R*_f 0.18) has the bridges to the cyclophane on opposite sites of the porphyrin ring which, as a result, is located within the macrocyclic cavity. CPK-Model examinations show that this geometry is sterically disfavored and requires some distortion of the porphyrin. Heating of the atropisomer mixture in refluxing toluene or *p*-xylene resulted in the quantitative conversion of the undesired minor atropisomer into the desired major atropisomer **2**.

Quantitative demetallation of **2** to **1** was achieved by stirring a solution of the zinc(II) porphyrinate in conc. HCl/MeOH. In the free-base form of the porphyrin, the undesired minor atropisomer was again readily converted into the desired atropisomer **1** by heating in toluene or *p*-xylene. The Fe^III derivative was formed by treating **1** with ferrous bromide in refluxing THF; to avoid formation of μ-oxo dimers, the iron(III) porphyrinate was isolated as the bis(hydrobromide) salt **3** which could be recrystallized (see *Exper. Part*).

We initially anticipated that oxidations catalyzed by **3** (*Scheme 1*) could proceed according to two competing mechanisms: supramolecular catalysis with transfer of the O-atom from the high-valent oxo-iron intermediate to the substrate bound in the cyclophane cavity, or transfer of the O-atom in a bimolecular reaction at the open porphyrin side. Since such competition could complicate analysis of the supramolecular process, we prepared the μ-oxo dimer **4** in which the iron(III) porphyrinate is accessible only through the binding cavity.

The remarkably soluble μ-oxo dimer **4** was obtained by stirring a solution of **3** in CH₂Cl₂/10% NaOH solution. Progress of the formation of the μ-oxo dimer **4** was conveniently monitored by UV/VIS spectroscopy (see *Fig. 3*, below).

2.2. *^{1}H-NMR Spectroscopy of the Porphyrin-cyclophanes.* Readily assignable ^{1}H-NMR spectra of the zinc(II) porphyrinate **2** in *p*-(D_{10})xylene were only obtained at temperatures above 100° where rotation about the two amide bonds in **2** becomes fast on the ^{1}H-NMR time scale (see *Fig. 1*). The ^{1}H-NMR spectra of the Fe^{III} derivatives **3** and **4** differ dramatically from those of **1** and **2** as a result of the paramagnetism of the d^5 metal ion [24]. The spectrum of **3** recorded in CDCl$_3$ at 22° (*Fig. 2*) shows extremely broad and shifted peaks as a result of the coupling of the protons with the unpaired electrons of the Fe-atom [24]. This coupling occurs both through bonds ('contact shifts') and through space ('dipolar' or 'pseudocontact' shifts). The sum of these effects is known as the isotropic shift, ΔH^{iso}, and is equal to the difference in shift between the paramagnetic and an analogous diamagnetic compound. One other characteristic of paramagnetic iron porphyrinates is extremely short relaxation times ($T_1 = 3$–$9 \cdot 10^{-11}$ s), which allows for
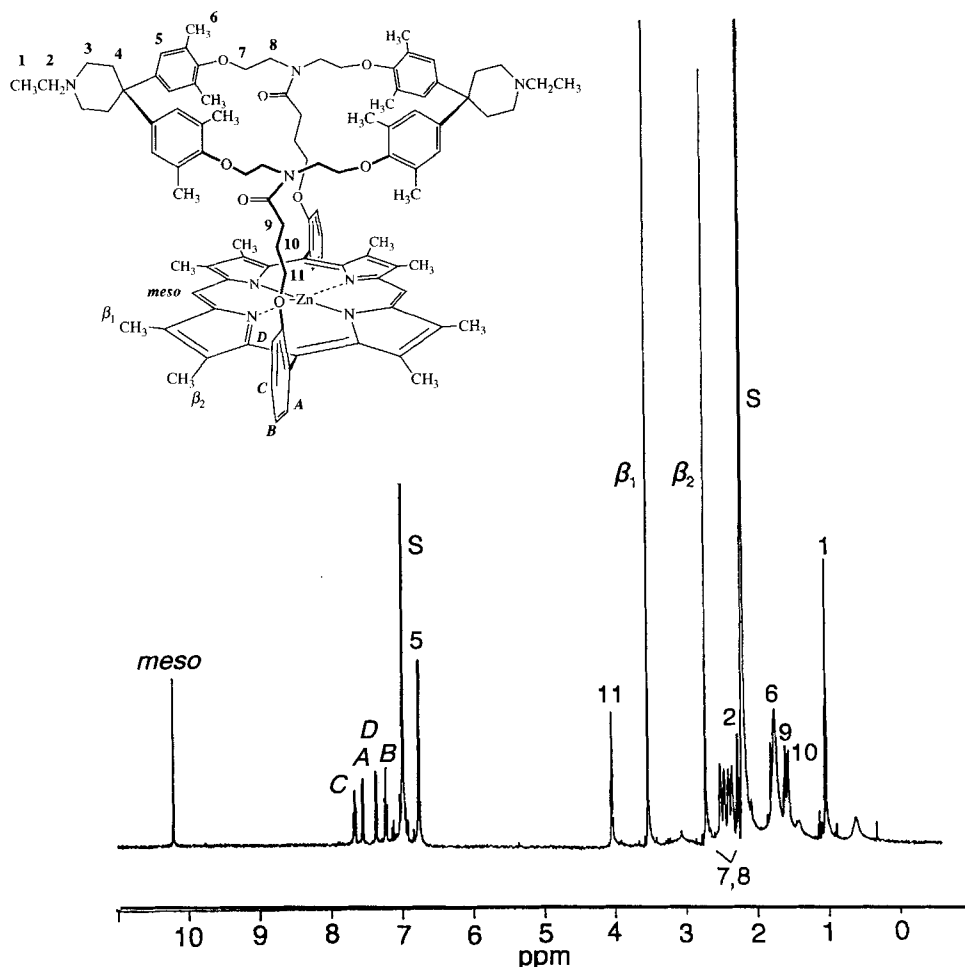

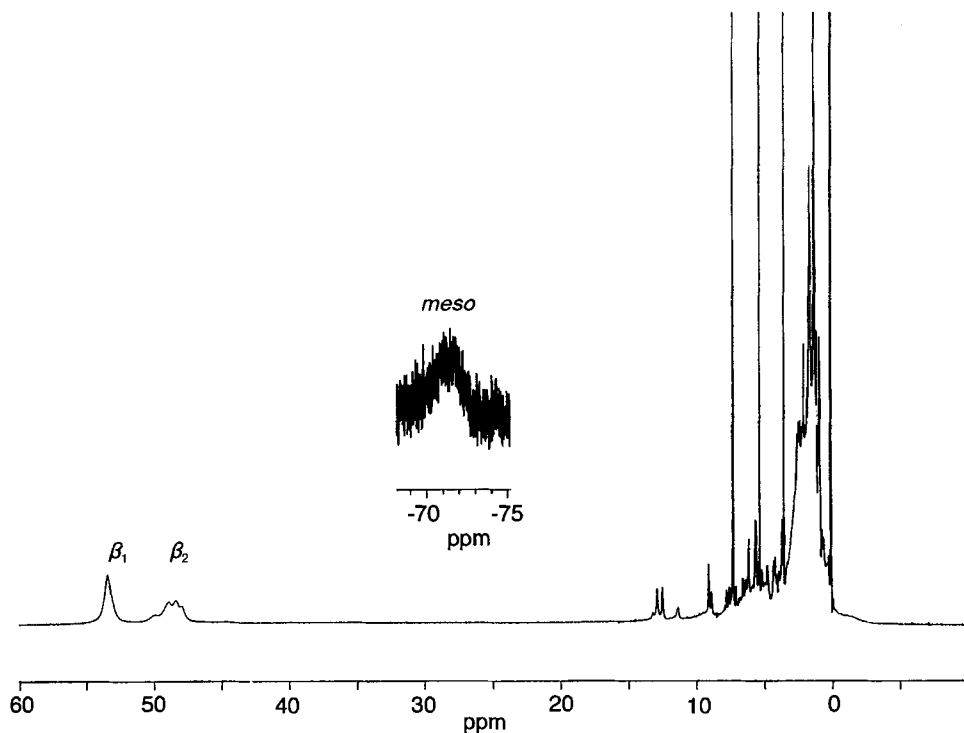Fig. 1. *500-MHz ^{1}H-NMR Spectrum of* **2** *in* p-(*D_{10}*)*xylene. T* 383 K; S = solvent; arbitrary numbering.

Fig. 2. *500-MHz ^{1}H-NMR Spectrum of* **3** *in CDCl$_3$. T* 295 K; for numbering, see *Fig. 1.*

very short acquisition times in ^{1}H-NMR experiments. The peaks centered at 48 and 54 ppm (*Fig. 2*) are assigned to the Me—C(β) groups of **3**, while the extremely broad peak at −74 ppm is due to the *meso*-protons. The temperature dependence of the chemical shift serves as one criterion for assigning paramagnetically shifted protons: both downfield and upfield shifts are magnified when the temperature of the sample is lowered. *E.g.*, at room temperature (22°), the Me—C(β) groups of **3** in CD$_3$OD appear as two separate signals at 60 and 73 ppm; on lowering the temperature to −69°, they are shifted even further downfield, ending up at 107 and 130 ppm, respectively. The *meso*-protons can not be detected under these conditions. From the isotropic shifts of the *meso*-protons and Me—C(β) groups, the iron(III) porphyrinate **3** is assigned as high-spin ($S = 5/2$) complex [24]. The complexity of the signals of **3** between 0 and 10 ppm does not allow to extract more structural information.

In the ^{1}H-NMR spectrum of the μ-oxo dimer **4** in CDCl$_3$ at room temperature, the downfield-shifted resonances have disappeared as a result of antiferromagnetic coupling of the two high-spin Fe-atoms *via* the oxo bridge [24b]. When the spectrum is recorded in CD$_3$OD, however, two broad humps appear reproducibly at 37 and 43 ppm, indicating reduced antiferromagnetic coupling in this solvent. As shown below, μ-oxo dimer **4** is stable in CD$_3$OD with respect to dissociation into two monomeric high-spin compounds. In contrast, **4** is in rapid equilibrium with two high-spin monomers in CF$_3$CH$_2$OH. Correspondingly, the ^{1}H-NMR spectrum of **4** in CF$_3$CD$_2$OD shows two broad down-

field-shifted peaks with strongly concentration-dependent chemical shifts. At low concentration, they appear in the positions expected for the Me—C(β) groups of the monomeric high-spin compound.

2.3. *UV/VIS Spectroscopy of the Porphyrin-cyclophanes.* In addition to causing interesting ring-current effects in the ^{1}H-NMR spectra, the extended annulene skeleton of porphyrins also produces characteristic optical spectra [25]. The UV/VIS spectra of **1–4** in CH$_2$Cl$_2$ (*Figs. 3a–d*) agree well, both in λ_{max} and ε values, with those published by *Baldwin* and coworkers for other bridged octamethyl-*meso*-diphenyl-porphyrins [20a]. The most intense absorption is the *Soret* band, a π-π* transition usually between 400 and 420 nm with a molar extinction coefficient (ε) usually greater than 10^5 l mol^{-1} cm^{-1}. Most structural information on porphyrins is obtained from the less intense, longer-wavelength absorptions between 500 and 700 nm. In the spectrum of **1** (*Fig. 3a*), four major bands are observed in the long-wavelength region at 628 (lg ε 3.10), 576 (3.78), 541 (3.69), and 507
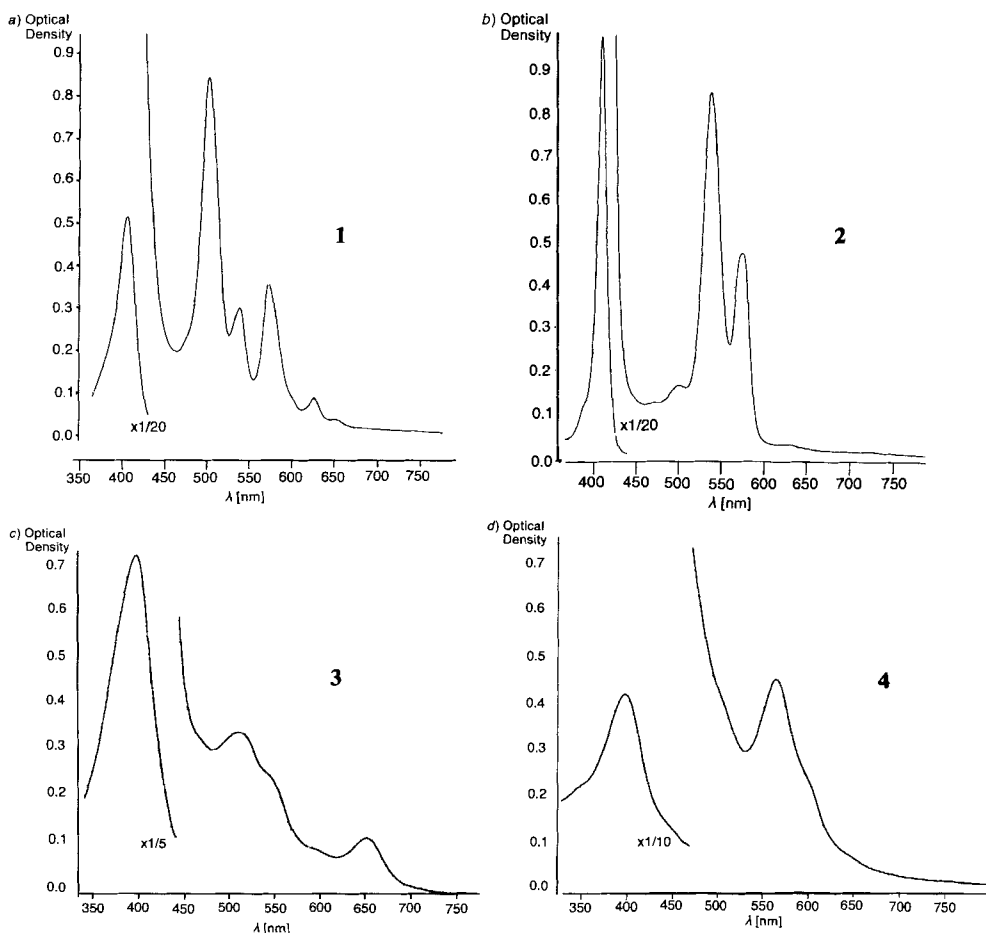

Fig. 3. *UV/VIS Spectra of* a) **1** ($c = 5.8 \cdot 10^{-5}$ mol l^{-1}), b) **2** ($c = 5.4 \cdot 10^{-5}$ mol l^{-1}), c) **3** ($c = 3.9 \cdot 10^{-5}$ mol l^{-1}), *and* d) **4** ($c = 6.9 \cdot 10^{-5}$ mol l^{-1}) *in CH$_2$Cl$_2$. T* 295 K; $d = 1$ cm.

(4.16) nm, and this absorption pattern is typical for metal-free porphyrins. The zinc porphyrinate **2** (*Fig. 3b*), shows only three longer-wavelength π-π* absorptions at 575 (lg ε 3.95), 539 (4.20), and 502 (3.49) nm. The missing band at 628 nm (*cf.* **1**) provides a convenient tool for monitoring the progress of zinc insertion. The longer-wavelength absorptions of Fe^{III} derivative **3** (*Fig. 3c*) appear at 652 (lg ε 3.45), 589 (sh, 3.40), 540 (sh, 3.81), and 507 (3.94) nm and the *Soret* band (394 nm, lg ε 4.97) at significantly shorter wavelength in comparison to **1** (409 nm, lg ε 5.25) and **2** (411 nm, lg ε 5.47). The concentration dependence of the *Soret* band in MeOH and CF$_3$CH$_2$OH suggests that **3** aggregates at higher concentrations in these solvents.

To investigate whether the axial ligand of **3** in protic solvents is bromide or rather a solvent molecule, we prepared an analog of **3** having SbF$_6^-$ as a non-coordinating axial ligand. Identical UV/VIS spectra and ^{1}H-NMR spectra of **3** and the analog **3**(3 SbF$_6^-$ instead of 3 Br$^-$) in CF$_3$CH$_2$OH and MeOH strongly suggest that in both solvents the original ligand has been removed from the Fe-atom.

Prior to investigations of monooxygenase activity of μ-oxo dimer **4**, we needed to prove that **4** is a kinetically stable species in protic solvents, where apolar cavity inclusion is most efficient. The UV/VIS spectra provided conclusive evidence that the μ-oxo dimer **4** is a stable species in MeOH. The spectrum of the μ-oxo dimer [25c] in MeOH has a *Soret* band at 404 nm (lg ε 5.23) and long-wavelength transitions at 598 (4.00), 576 (3.98), and 486 (4.24) nm. The missing long-wavelength band of **3** at 652 nm provides a convenient tool for monitoring the progress of formation of **4**. However, in CF$_3$CH$_2$OH, **4** shows UV/VIS absorptions identical to those of low concentrations of **3** in the same solvent. This indicates that dimer **4** is unstable in CF$_3$CH$_2$OH and dissociates to the monomers.

Under acidic conditions, **4** completely dissociates into the monomeric species. Indeed, the UV/VIS spectrum of **4** in MeOH containing two drops of 2% HBr solution is identical in all respects to that of **4** in CF$_3$CH$_2$OH and to the low-concentration spectrum of **3** in MeOH. Pure MeOH is not acidic enough (pK_x 15.5) to induce dissociation, whereas the pK_x of the more acidic CF$_3$CH$_2$OH apparently is low enough (pK_x 12.4) to lead to protonation of the oxo bridge (O^{2-}) in **4** and subsequent dissociation.

2.4. *^{1}H-NMR Binding Studies with Porphyrin-cyclophane* **1**. Before assessing the supramolecular catalytic activity of the iron(III) porphyrinates **3** and **4**, it was necessary to demonstrate that such structures would form inclusion complexes with polycyclic aromatic hydrocarbons. Since the paramagnetism of the Fe^{III} derivatives prevented the use of ^{1}H-NMR binding titrations, such complexation assays were done with metal-free **1** in MeOH solution. Although **1** is poorly soluble in pure MeOH, it dissolves readily after protonation, and solubilities greater than 20 mM are achieved.

The complexation of naphthalene, acenaphthylene, pyrene, and phenanthrene by **1** was studied by ^{1}H-NMR spectroscopy in CD$_3$OD/D$_2$O/CD$_3$COOD 95:4.85:0.15 (v/v). The greater insolubility of anthracene required the addition of (CD$_3$)$_2$SO, *i.e.* the use of CD$_3$OD/(CD$_3$)$_2$SO/D$_2$O/CD$_3$COOD 90:5:4.85:0.15 (v/v). The 500-MHz ^{1}H-NMR titrations were carried out at 293 K employing a constant guest concentration, while the concentration of the host was varied to give *ca.* 20–90% saturation binding. The association constants K_a (l mol^{-1}) and free energies of complexation $-\Delta G°$ (kcal mol^{-1}) were obtained by nonlinear least-squares curve fitting of the complexation-induced changes in chemical shift of the guest protons ($\Delta\delta$) plotted against the host concentration. During

titrations, the upfield-shifted guest resonances were strongly broadened which is indicative of a decomplexation rate near the NMR time scale. *Fig. 4* shows the spectra recorded during the titration of phenanthrene with **1** and *Fig. 5* the calculated upfield complexation shifts at saturation binding ($\Delta\delta_{sat}$) of guest resonances that could be monitored over the
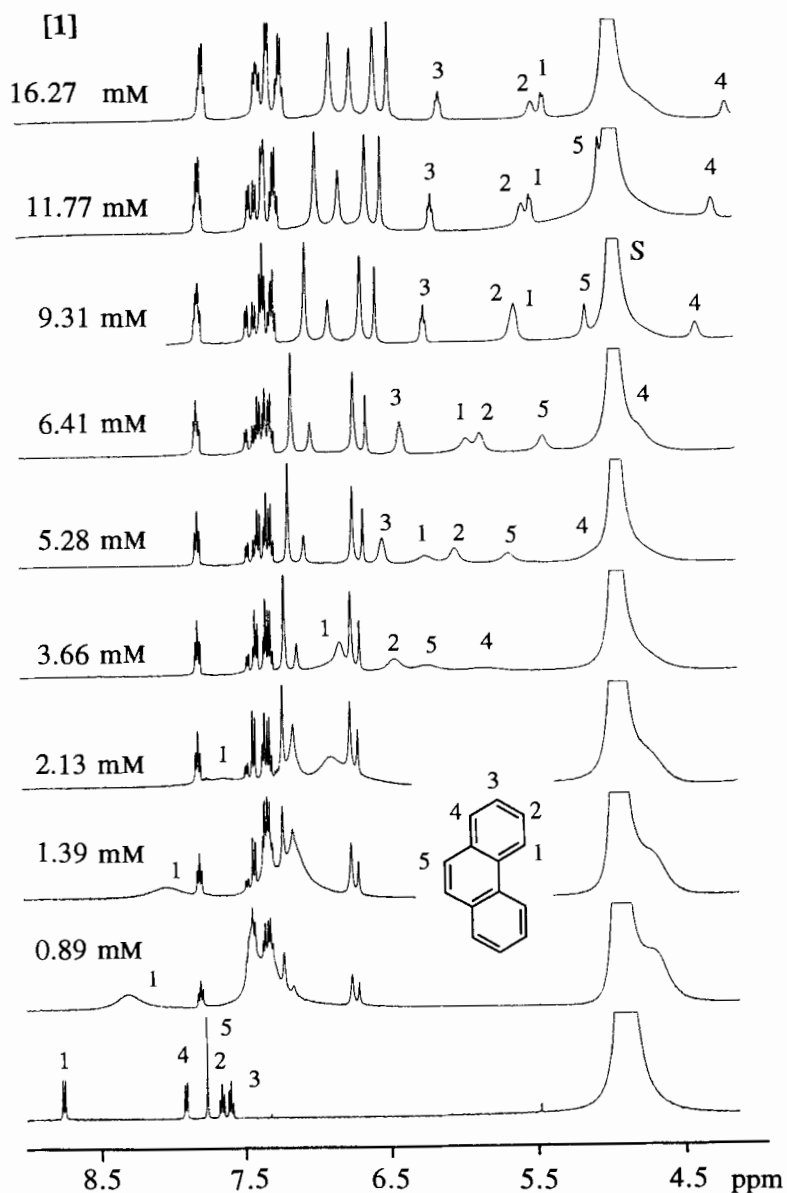

Fig. 4. *500-MHz ^{1}H-NMR Titration of phenanthrene ($c = 5.2$ mM) with **1** ($c = 0.88$–12.9 mM) in $CD_3OD/D_2O/CD_3COOD$ 95:4.85:0.15. T 293 K; S = solvent.*
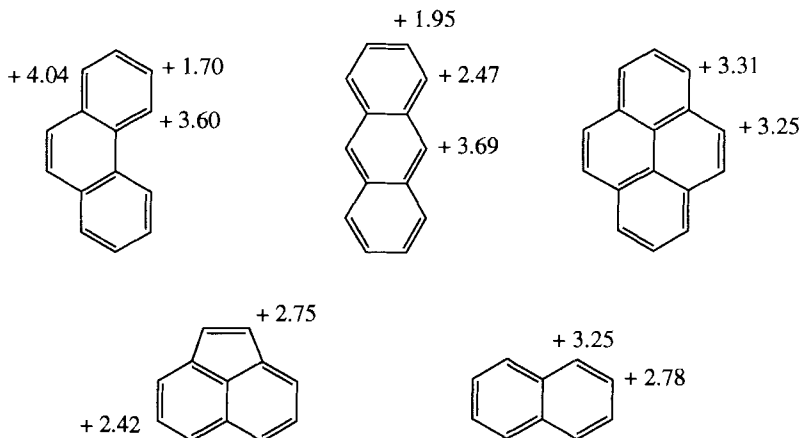
Fig. 5. *Calculated upfield complexation shifts* ($\Delta\delta_{sat}$) *of observable guest* ^{1}H-NMR *signals in complexes of* 1 *at saturation binding*

Table 1. *Association Constants* K_a *and Binding Free Energies* $-\Delta G°$ *for the Polycyclic Aromatic Hydrocarbon Complexes of* 1 *in* $CD_3OD/D_2O/CD_3COOD$ 95:4.85:0.15 (v/v). T 293 K[a]).

Guest	Phenanthrene	Acenaphthylene	Anthracene[b])	Naphthalene	Pyrene
K_a [l mol^{-1}]	1330	1050	460	330	160
$-\Delta G°$ [kcal mol^{-1}]	4.19	4.05	3.57	3.38	2.95

[a]) Accuracy of the K_a values: ±10%. [b]) In $CD_3OD/(CD_3)_2SO/D_2O/CD_3COOD$ 9:5:4.85:0.15 (v/v).

entire titration range. The K_a and $\Delta G°$ values in *Table 1* are averages of the data obtained by individual evaluation of the complexation-induced shifts of all observable guest resonances.

Upon complexation, the ^{1}H-NMR signals of the bound guest move strongly and differentially upfield, whereas the aromatic diphenylmethane protons of 1 move downfield. Such complexation-induced shifts are highly characteristic of inclusion complexation by [n.1.n.1]paracyclophanes [17]. The upfield shifts $\Delta\delta_{sat}$ of the guest resonances at saturation binding, some > 4 ppm (*Fig. 5*), are considerably larger than those normally observed in the complexes of similar cyclophanes that are not bridged by a porphyrin ($\Delta\delta_{sat} = 1-2.5$ ppm). In the complexes of 1, the guest protons are not only exposed to the shielding cyclophane cavity but also to the strongly shielding region of the planar porphyrin ring [26]. Under slow host-guest exchange conditions, some of the upfield shifts would be even larger. CPK-Model examinations suggest that phenanthrene, like pyrene and anthracene, prefers an 'axial' orientation in the cavity (*Fig. 6a*) which exposes one end of the molecule directly to the porphyrin plane while the other end is projecting from the mouth of the host. On the time scale of our NMR experiments, bound phenanthrene rapidly exchanges position *via* decomplexation-recomplexation and the protons at its two ends resonate at the average of the chemical shifts for these two different environments. Under slow host-guest exchange conditions, much stronger upfield shifts would be observed for those protons that are directly exposed to the porphyrin plane.
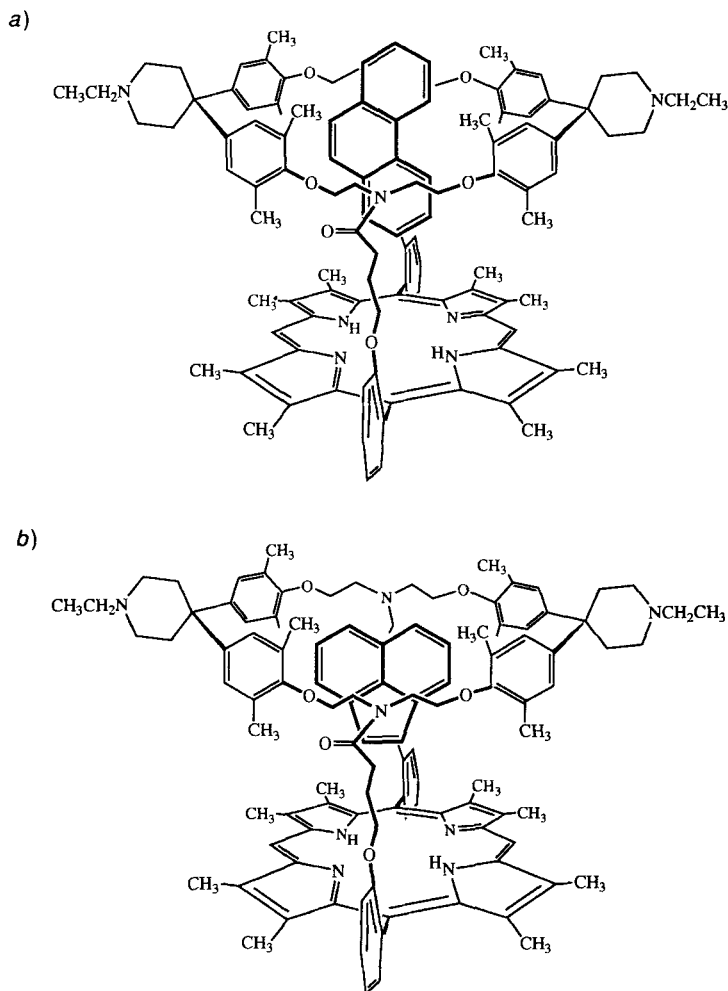
a)

b)

Fig. 6. *Favorable geometries of the complexes formed by* 1 *with* a) *phenanthrene and* b) *acenaphthylene*. The geometries shown are supported by CPK-model examinations, computer-modelling studies, and by the complexation-induced shifts in the ^{1}H-NMR spectra.

In addition to characteristic complexation-induced shifts, other evidence for cavity binding of polycyclic aromatic hydrocarbons to 1, as opposed to π-π stacking on the open face was obtained. On the ^{1}H-NMR time scale at 293 K, host 1 exists as two conformers due to different orientations of the two amide bonds in the straps which connect the porphyrin with the cyclophane moiety and, as a result, the aromatic diphenylmethane protons are split into several peaks (*Fig. 4*). During the titration, changes in the relative intensity of these peaks are observed which suggests that one of the two possible amide rotamers is favored in the host-guest complexes. Such changes would not occur if binding simply resulted from π-π stacking at the open porphyrin face. When compound 12

12

13
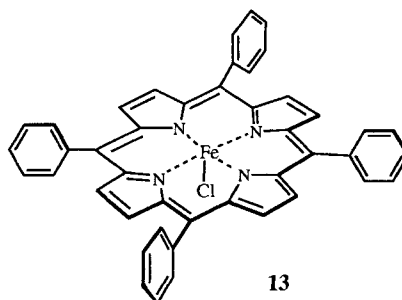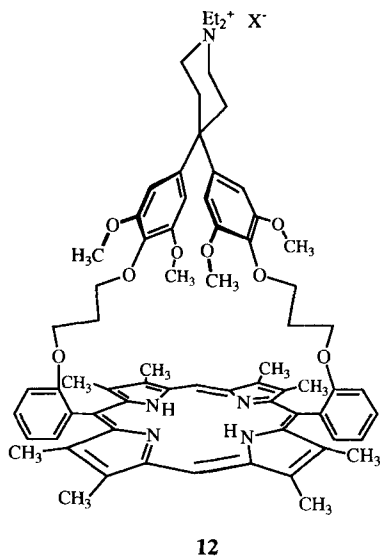
[26] ($c = 5$ mM) which has an identically strapped porphyrin as in **1**, but which lacks an efficient organized binding site, is added to phenanthrene (5 mM) or naphthalene (5 mM) in the methanolic solvent mixture, no shifts of the host protons are observed, except for a 0.1-ppm shift of the phenanthrene d of H–C(1) at 8.75 ppm. In contrast, complexation by **1** in the same concentration range shifts this resonance by more than 2 ppm.

The relative stability of the complexes formed between **1** and the aromatic hydrocarbons (*Table 1*) does not parallel the size of the apolar surface of the guest, but can be explained with the help of CPK-model examinations and by taking into account previous experiences with [$n.1.n.1$]paracyclophane receptors [17]. All guests except pyrene can adopt an orientation in the cavity in which they undergo π-π stacking interactions with one pair of parallel aromatic rings of the host and edge-to-face interactions with the other pair. Pyrene is too large and can only be incorporated into the plane which passes through the two spiro centers and runs perpendicular to the mean plane of the cyclophane [17]. In such an orientation, aromatic-aromatic interactions are reduced and a weaker complex is formed. 'Equatorially' bound acenaphthylene and 'axially' bound phenanthrene show the best fit to the cavity and form the most stable complexes. Anthracene binds in an 'axial' orientation which allows a significant amount of lateral motion, and naphthalene is not large enough to fill the entire binding site; hence, the complexes of these two guests are less stable.

The structural assignments based on CPK molecular model examinations found further support in molecular-modelling studies with the MM2 force-field implemented into the Macromodel program V2.6 [27]. In the search for favorable conformations of the [**1** (acenaphthylene)] complex, the guest consistently sank deeply into the cavity and always took an 'equatorial' position which approaches its most reactive 1,2-double bond to the plane of the porphyrin moiety as shown schematically in *Fig. 6b*. In the phenanthrene complex, the guest molecule was exclusively found in an 'axial' position which locates its reactive 9,10-double bond far from the porphyrin site. In both complexes, the

straps between the porphyrin and the cyclophane moieties prefer adopting extended conformations, and the porphyrin moiety is found preferentially in positions where its edges can make additional hydrophobic contacts with the diphenylmethane spacers.

2.5. *UV/VIS Binding Studies with 1 and 3*. When phenanthrene was added to a solution of **1** in MeOH or CF_3CH_2OH, the UV/VIS spectrum of the porphyrin-cyclophane showed a marked change in its VIS absorption bands. The *Soret* band was most affected, and its absorbance was significantly reduced in the presence of the guest. A similar effect was also observed with the Fe^{III} derivative **3** which, in this case, can be attributed in part to a change in the polarity around the Fe-atom [25b]. *Fig. 7* shows a
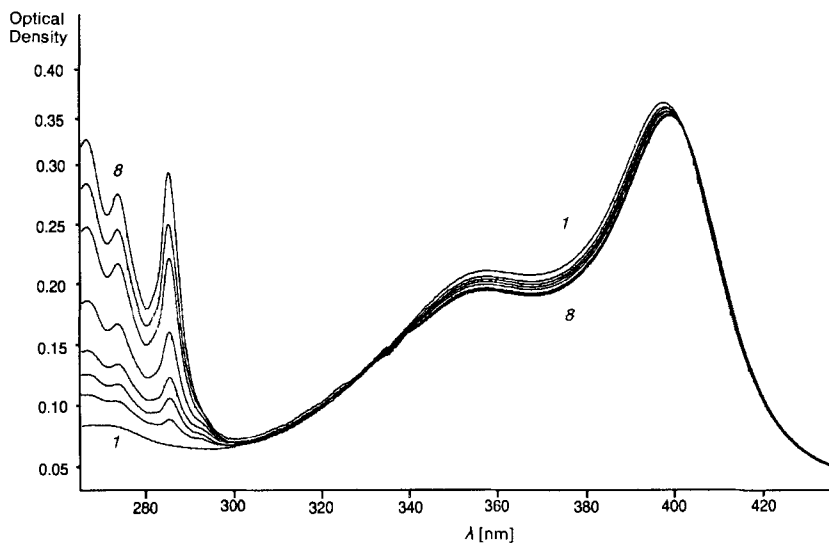

Fig. 7. *UV/VIS Titration of* **3** ($c = 2.0 \cdot 10^{-5}$ mol l^{-1}) *with phenanthrene* (spectrum *1*: $c = 1.4 \cdot 10^{-5}$ mol l^{-1}; spectrum *8*: $1.0 \cdot 10^{-4}$ mol l^{-1}) *in* CF_3CH_2OH *at 293 K. d = 1 cm.*

UV/VIS binding titration in CF_3CH_2OH in which the decrease in intensity of the *Soret* band of **3** ($c = 2.0 \cdot 10^{-5}$ mol l^{-1}) was monitored as a function of increasing phenanthrene concentration ($c = 1.4 \cdot 10^{-5}$ to $1.0 \cdot 10^{-4}$ mol l^{-1}); a clean isosbestic point was observed at 408 nm. The measured K_a for this complex is 39400 l mol^{-1}, which corresponds to a binding free energy $\Delta G^\circ = -6.2$ kcal mol^{-1}. A titration of **1** ($c = 1.8 \cdot 10^{-5}$ mol l^{-1}) with phenanthrene ($c = 1.0 \cdot 10^{-4}$ to $1.0 \cdot 10^{-3}$ mol l^{-1}) in pure MeOH gave a K_a value of 1500 l mol^{-1} ($\Delta G^\circ = -4.3$ kcal mol^{-1}), in nice agreement with the value obtained by ^{1}H-NMR (*Table 1*). The large increase in stability of 1.9 kcal mol^{-1} measured for the phenanthrene complex of **3** in CF_3CH_2OH, as compared to the same complex of **1** in MeOH, was expected from the solvent dependency of tight apolar complexation strength that had previously been established in studies with cyclophane receptors and aromatic-hydrocarbon guests [17] [21].

2.6. *Electron Spin Resonance (ESR) and Electrochemical Studies of* **3**. It is known that camphor (cam) binding increases the reduction potential of $P-450_{cam}$ from -300 mV to -170 mV [11]. The X-ray crystallographic work by *Poulos* and coworkers [10] has

provided a structural basis for this change. In substrate-free P-450$_{cam}$, the binding cavity is filled with H_2O molecules, one of which is ligated to the Fe-atom, possibly as a OH group. Under these conditions, the heme experiences a high dielectric environment which serves to stabilize the ferric form of the enzyme. Binding of camphor displaces all solvent from the cavity, including the molecule ligated to the Fe^{III} center. Under these less polar conditions, reduction to the Fe^{II} state becomes more favorable. Such modulation of the redox potential by a microenvironment was also found in nonenzymatic iron-porphyrinate systems [28], and we were interested in evaluating possible effects of substrate binding on the reduction potential of 3.

The cyclic voltammograms of MeOH solutions of 3 show three main reduction waves, but there is no well defined anodic peak (*Fig. 8*). Repeated scans establish that the absence of the reverse anodic peaks is not due to passivation of the electrode. When the tight binders phenanthrene or acenaphthylene were added to the solution, no significant changes in the cyclic voltammogram of 3 occurred (*Fig. 8*). Even though the formal potential cannot be estimated due to the irreversibility of the system, the results nevertheless show that there is no significant change in the reduction potential. This suggests that, even though phenanthrene and acenaphthylene bind strongly to 3, they are not bound deeply enough in the cavity to displace all the solvent molecules or induce any significant change in the coordination sphere of the metal center, changes that would affect the reduction potential.
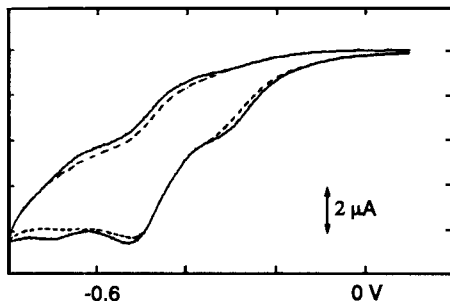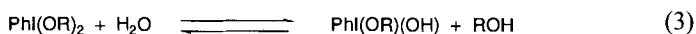

Fig. 8. *Cyclic voltammograms of* 3 (*c* = 4.76 mM) *in MeOH* (0.1M LiCl, 0.06M HCl) *at 20° in the absence* (– – –) *and presence* (——) *of acenaphthylene* (*c* = 43 mM). *Scan rate* 0.1 V s^{-1}.

An ESR titration of P-450$_{cam}$ with camphor revealed that substrate binding also induces a change in the spin state of the Fe^{III} atom from low ($S = 1/2$) to > 95% high ($S = 5/2$) spin [29]. In the substrate-free form, the low-spin state is favored whereas upon camphor binding, displacement of the solvent and the axial aqua ligand leads to the formation of a pentacoordinate heme-iron, shifting the spin equilibrium to the high-spin form. As with the reduction potential, the spin state of the Fe-atom is dependent on the local solvation state of the heme. *Fisher* and *Sligar* found a linear free-energy relationship linking the spin-state equilibrium with the change in the redox potential of P-450$_{cam}$ [30]. In supramolecular chemistry, a change in spin equilibrium upon substrate binding was observed in an iron(III) porphyrinate sandwiched between two cyclodextrins [19h], a change we hoped to see in complexation of aromatic hydrocarbons by 3.

ESR Studies were conducted at 10 K on frozen solutions of **3** ($c = 1.9 \cdot 10^{-3}$ mol l^{-1}) alone in CF_3CH_2OH and in the presence of acenaphthylene ($c = 1.04 \cdot 10^{-2}$ mol l^{-1}), phenanthrene ($c = 1.02 \cdot 10^{-2}$ mol l^{-1}), or imidazole ($c = 2.08 \cdot 10^{-2}$ mol l^{-1}) [31]. The spectrum of **3** showed that this compound exists exclusively in the high-spin state ($g \approx 6$) under these conditions, both in the presence and absence of the guest. This result is in agreement with the findings of the NMR study (see *Chapt. 2.2*). Only the spectrum of the solution containing an excess of imidazole gave a signal expected for a low-spin Fe^{III} state. Similar results were obtained on solid samples of **3** alone and in the presence of the aromatic hydrocarbons or imidazole. All experiments showed that the iron(III) porphyrinate **3** exists exclusively in the high-spin form in the absence of N-containing bases. It seems that to model the spin-state equilibrium of cytochrome P-450 enzymes, a strong axial donor ligand such as the enzymatic thiolate ligand is required to force the Fe^{III} into the low-spin state.

2.7. *Supramolecular Catalysis of Oxidation Reactions.* 2.7.1. *General.* To explore the catalytic potential of the iron(III) porphyrinate **3** and the μ-oxo dimer **4**, we investigated the epoxidation of acenaphthylene in CF_3CH_2OH using iodosylbenzene (PhIO) as the O-transfer agent. Acenaphthylene forms a stable complex, and computer modelling (*Chapt. 2.4*) had suggested that its reactive 1,2-double bond prefers to orient in a productive way towards the iron porphyrinate. The 1,2-bond in acenaphthylene has a *Hückel* bond order of 0.796, which is midway between an aromatic (0.667) and an olefinic C=C bond (1.00) [32]. Therefore, it should be more activated than a regular benzenoid double bond. CF_3CH_2OH was chosen as the solvent since it favors strong host-guest complexation and since it was found by *Traylor* to be more stable against oxidation than MeOH [33].

It was of particular interest to study supramolecular catalysis by **3** and **4** under homogeneous reaction conditions in a protic solvent, since almost all previous epoxidations using iron(III) porphyrinates and iodosylbenzene (PhIO) had been performed under heterogeneous reaction conditions in aprotic organic solvents such as CH_2Cl_2. The use of protic solvents usually was prevented due to limited solubility of simple porphyrins in such environments. In CH_2Cl_2 and other aprotic solvents, PhIO exists as an insoluble polymeric material [34]. In alcoholic solvents, however, polymeric PhIO undergoes solvolysis to give a soluble dialkoxy(phenyl)iodamethane (*Eqn. 2*) which, in the presence of H_2O, is in equilibrium with a hemiacetal-type species (*Eqn. 3*) [34]. *Traylor et al.* reported that addition of $MeOH/H_2O$ or CF_3CH_2OH/H_2O to oxidation mixtures consisting of iron(III) porphyrinates and pentafluoroiodosylbenzene in CH_2Cl_2 led to tremendous rate accelerations as a result of the formation of soluble $PhI(OH)(OR)$ species and homogeneous reaction conditions [35]. Only one study of iron-porphyrinate-mediated oxidations under homogeneous conditions in a pure hydroxylic solvent was reported [36].

$$\left(O{\diagdown}I{\diagup}O{\diagdown}I{\diagup}O\right)_n \quad \xrightarrow{ROH} \quad 2n \; RO{\diagdown}I{\diagup}OR \tag{2}$$

PhI(OR)$_2$

$$PhI(OR)_2 + H_2O \;\rightleftharpoons\; PhI(OR)(OH) + ROH \tag{3}$$
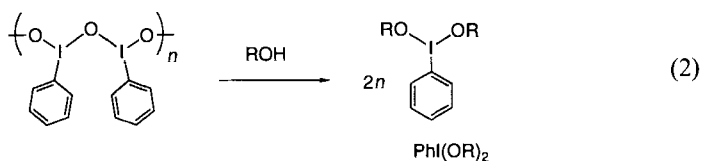
In that work, [tetra(1-methylpyridin-4-io)porphyrinato]iron(III) was used with PhIO in MeOH to catalyze olefin epoxidations and anisole demethylations. The measured yields were similar to those obtained in aprotic solvents under heterogeneous conditions. Epoxidations could also be carried out in H_2O, but the low solubility of the alkenes and an increase in allylic hydroxylation at the expense of alkene epoxidation rendered these conditions undesirable.

2.7.2. *Catalysis of Acenaphthylene Oxidation.* In addition to preparative-scale runs which were subsequently worked up for product isolation, most catalytic studies described in the following involved analytical runs which were analyzed by gas chromatography (GC) of the crude reaction mixtures. When homogeneous solutions of acenaphthylene (*ca.* 10 mM), PhIO (*ca.* 15 mM), and catalyst **3** or **4** (*ca.* 0.5 mM) in CF_3CH_2OH were stirred at 295 K (*Runs 1* and *3* in *Table 2*), TLC analysis instantaneously showed the appearance of two intensely blue fluorescent spots (SiO$_2$, CH$_2$Cl$_2$, R_f = 0.63 and 0.41).

Table 2. *Oxidation of Acenaphthylene to Acenaphthen-1-one* (**14**) *catalyzed by the Iron(III) Porphyrinates* **3**, **4**, *and* **13** *at 295 K in the Presence of PhIO as Oxygen Transfer Agent*[a])

Run	Catalyst		Solvent	Ace-naph-thylene [mM]	PhIO [mM]	Inhibitor phenan-threne [mM]	Yield of **14** [%][b])	Turn-over number[c])	Unreacted acenaph-thylene [%]
	type	concen-tration [mM]							
1	3	0.54	CF$_3$CH$_2$OH	11	15	–	28 (26[d])	6	[e])
2	3	0.54	CF$_3$CH$_2$OH	12	15	11	14 (14[d])	3	[e])
3	4	0.49	CF$_3$CH$_2$OH	13	13	–	20.5	5.4	42
4	4	0.49	CF$_3$CH$_2$OH	13	13	10.4	14.7	3.9	51
5	–	–	CF$_3$CH$_2$OH	12.3	14	–	2.5	–	75
6	13	1.3	CH$_2$Cl$_2$/CF$_3$CH$_2$OH	11.2	14	–	14	1.2	49
7	13	1.3	CH$_2$Cl$_2$/CF$_3$CH$_2$OH	11.4	14	11.0	14	1.2	52
8	4	0.19	MeOH	11.8	12.0	–	28	9	59
9	13	0.44	MeOH/CH$_2$Cl$_2$ 6:4	12.4	18.5	–	11.3	3.2	72
10	–	–	MeOH	11.8	12.0	–	< 1	–	84

[a]) All reactions were protected from light and O_2. Workup after 3 h; in most runs, all porphyrin was bleached after 30 min. [b]) Yields based on initial acenaphthylene concentration and determined by calibrated GC integrations. [c]) Turnover number = mole of acenaphthylene converted per mole of catalyst. [d]) Yields of isolated product determined from UV/VIS spectra. [e]) Not determined.

Over time, the less polar spot converted completely into the more polar one and, after *ca.* 30 min, the mixture did not show any more changes since the porphyrin catalyst was completely bleached. The more polar product was isolated and identified by ¹H-NMR, MS, and IR as acenaphthen-1-one [37] (**14**; *Scheme 3*). The initially formed less polar compound was identified as epoxide **15**, which was independently prepared by oxidation of acenaphthylene with 3-chloroperbenzoic acid [38]. We propose that the formation of **14** in the iron-porphyrinate-catalyzed oxidations arises *via* acid-catalyzed rearrangement of the initially formed epoxide **15** (*Scheme 3*). Epoxide **15** does not survive GC analysis at an injection port temperature of 150° [38a]; it undergoes thermal isomerization to **14**.

For comparison and calibration of response factors in the GC product analysis of crude reaction mixtures, **14** was initially obtained preparatively in 58% yield (turnover

Scheme 3. *Iron-Porphyrinate-Catalyzed Oxidation of Acenaphthylene to Acenaphthen-1-one* (**14**)
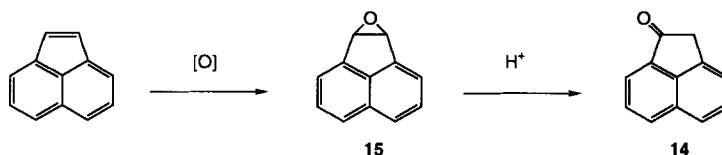
number = 11) by catalytic oxidation of acenaphthylene (23 mM) with PhIO (32.0 mM) in CH_2Cl_2/CF_3CH_2OH 5:2 in the presence of the iron(III) tetraphenylporphyrinate **13** (1.2 mM; see above). This represents the shortest and highest-yielding preparation of **14** [37]. The same reaction in pure CH_2Cl_2 yielded 40% of **14** (turnover number = 7), a much higher yield than had been previously reported [16c].

Due to the very different solubility characteristics of **3** and **4** *vs.* **13**, the advantages of supramolecular catalysis by **3** and **4** could not be determined from comparative runs under identical conditions in pure CF_3CH_2OH. However, in CH_2Cl_2/CF_3CH_2OH 1:1, the catalytic activity of **13** was found to be much lower than the activity of **3** and **4** in pure CF_3CH_2OH (*Runs 1, 3,* and *6, Table 2*). All reactions in the absence of porphyrin catalyst led to very small conversions to product (*Runs 5* and *10*).

Although binding studies with **1** and **3** suggest that the catalytic oxidation of acenaphthylene in the presence of the porphyrin-cyclophanes occurs within the cyclophane cavity, a reaction at the open porphyrin face was not easily excluded for **3** and even not for **4**. As shown above in *Chapt. 2.2* and *2.3*, the μ-oxo dimer **4** is in rapid equilibrium with two monomers in CF_3CH_2OH, hence the reaction could occur on the open face of the porphyrin. One argument in favor of the supramolecular process could be the preference for a polar solvent molecule to coordinate axially during formation of the high-valent oxo species on the polar open face rather than on the apolar cavity side. CPK-Model examinations indicate that intra-cavity O-atom transfer from PhIO to the Fe^{III} can occur by two mechanisms. The O-atom may be delivered from PhIO while this compound is weakly bound in the cyclophane cavity. For supramolecular oxidation to occur, this mechanism requires that the high-valent oxo species survives a rapid sequence of elementary steps consisting of *a*) complexation of PhIO in the cavity, *b*) donation of the O-atom to the Fe-atom, *c*) decomplexation of PhI, *d*) substrate complexation, and *e*) O-atom transfer to bound substrate. Alternatively, PhIO can transfer an O-atom by approaching the Fe^{III} center laterally through the openings between the cyclophane and the strapped porphyrin moieties while acenaphthylene is already bound in the cyclophane cavity. The latter mechanism would mimic cytochrome P-450 catalysis, where O-binding and activation is preceded by substrate binding (*Scheme 1*).

While acenaphthylene binds with its reactive 1,2-double bond in a productive orientation within the cavity of **3** and **4**, phenanthrene prefers forming an unproductive 'axial' complex (*Fig. 6*) in which its reactive $C(9)=C(10)$ bond is oriented away from the iron porphyrinate, which should prevent its facile oxidation in a supramolecular process. The oxidation of phenanthrene was indeed much more sluggish than the oxidation of acenaphthylene, and this strongly binding arene seemed, therefore, suitable to provide support for the intra-cavity catalytic process by demonstrating competitive substrate inhibition. In the presence of phenanthrene, yields of acenaphthen-1-one (**14**) in the

reactions catalyzed by **3** and **4** significantly decreased (*Runs 2* and *4*) while the yields of **14** in the reaction catalyzed by **13** remained unaffected (*Run 7*). A few percent of the phenanthrene in each run was converted to unidentified products.

Besides ketone **14**, a large fraction of unreacted acenaphthylene was recovered in all reactions (*Table 2*). Apparently, self-destructive oxidations of the catalyst are proceeding at a rate which is competitive to that of substrate oxidation. Acenaphthylene mass balances for oxidations in MeOH and, particularly in CF_3CH_2OH, were always far from optimal. A significant portion of material was unaccounted for in the GC integrations, even in the analysis of reactions without porphyrin catalyst (*Runs 5* and *10*). We tentatively propose the formation of mixed polymeric oxidation products consisting of acenaphthylene, iodosylbenzene, and solvent to account for the unidentified material that escaped GC analysis or liquid chromatographic isolation. In contrast to these findings, the mass balance for acenaphthylene oxidations under heterogeneous conditions in pure CH_2Cl_2 with **13** as the catalyst was in the range of 100%. Clearly, the oxidations in protic solvents need to be studied in greater depth to identify and subsequently prevent the reaction channels at the origin of the poor mass balances.

In the reactions catalyzed by **3**, **16**, and **17** (*Scheme 4*) were identified by GC/MS analysis as minor by-products which were not formed in the presence of **4** or **13**. Presumably, these products originate from the bromide counterions of **3** that are oxidized by $PhI(OH)(OR)$ to give hypobromous acid (HOBr). The Br^+ subsequently reacts with acenaphthylene to give a cyclic bromonium ion which is opened up by solvent to give **16**. Acid-catalyzed elimination of CF_3CH_2OH would yield 1-bromoacenaphthylene (**17**). If the initial product **16** is left standing in CF_3CH_2OH solution for 3 days, it is completely converted into **17**. Evidence for the proposed mechanism of formation of **16** and **17** was obtained from a control reaction. When acenaphthylene (66 mM) and PhIO (100 mM) were reacted with NH_4Br as source for Br^+ in CF_3CH_2OH at 295 K, products **16** and **17** were formed exclusively.

Scheme 4. *Possible Mechanism for Formation of HOBr and Reaction with Acenaphthylene in CF_3CH_2OH*
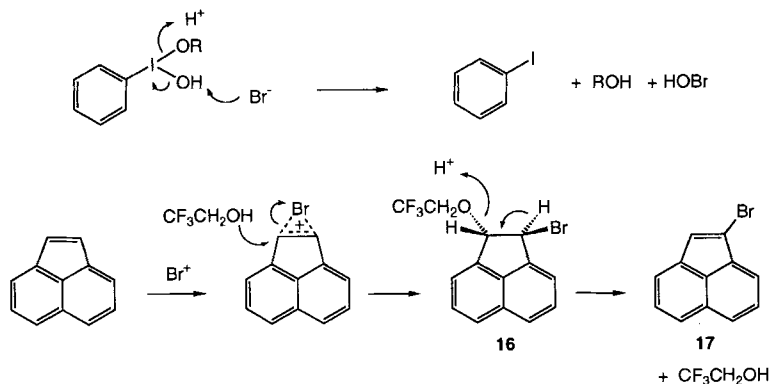
Strong evidence for effective supramolecular catalysis was finally obtained in the oxidation of acenaphthylene with **4** in MeOH where, as shown in *Chapt. 2.2* and *2.3*, the μ-oxo dimer is stable. *Chang* and *Kuo* had previously described intramolecular hydroxylations with a μ-oxo dimer, in which each of the two porphyrin moieties is strapped by a hydrocarbon chain [16a]. Oxidation of acenaphthylene by **4** in MeOH was very fast and gave a 28% yield of **14** which corresponds to a turnover number of 9 (*Run 8*). In a

control reaction without porphyrin (*Run 10*), less than 1% conversion to **14** was found. Mass balances in both reactions were much more favorable than for reactions in CF_3CH_2OH with only 13% of the initial acenaphthylene weight being unaccounted for in the GC integration. When tetraphenylporphyrin **13** was used under similar conditions in $MeOH/CH_2Cl_2$ 6:4 (*Run 9*), the yield after 30 min was 11.3% which translates to 3.2 turnovers. Thus, the oxidations with μ-oxo dimer **4** in MeOH not only provide convincing evidence for supramolecular reactivity, but the controls also suggest that this catalytic process in the cavity is superior to the reaction at the open face of a porphyrin moiety which does not involve a substrate-binding event.

2.7.3. *Aromatase Activity of* **3**. While we were trying to obtain evidence for supramolecular catalysis with **3** and **4** in CF_3CH_2OH, Professor *T. G. Traylor* suggested that we use isotetralin (= 1,4,5,8-tetrahydronaphthalene; **18**) as a probe [33]. He reasoned that if reaction occurred within the cavity, epoxidation of the less substituted double bonds would be favored over epoxidation at the central double bond which occurs with peracids. We found, however, that the preferred reaction pathway for **18** in the reaction with **3** was aromatization to give 1,4-dihydronaphthalene as the principal product, which was identified by GC-MS comparison with an authentic sample. To avoid the side reactions originating from **3** by formation of HOBr (see *Scheme 4*), the SbF_6^--ligated iron porphyrinate analogue **3**(3 SbF_6^- instead of 3 Br^-; 0.28 mM), was reacted with **18** (19 mM), and PhIO (15 mM) in CF_3CH_2OH to afford mainly 1,4-dihydronaphthalene (turnover number = 17), in addition to a minor amount of naphthalene, all residual material being starting **18**. This aromatization probably occurs *via* the O-rebound mechanism shown in *Scheme 5*. Reaction between the substrate and the oxoiron intermediate would generate a stabilized doubly α,β-unsaturated radical and a hydroxyiron(IV) intermediate. These would then combine to form the unstable hydrated dihydronaphthalene derivative which would immediately eliminate H_2O to give the observed product. Further investigations on this interesting aromatase activity of iron(III) porphyrinates in the presence of O-transfer agents are planned.

Scheme 5. *Possible Mechanism for the Aromatization of Isotetralin* (**18**) *in the Reaction with PhIO and* **3** *(3 SbF$_6^-$ instead of 3 Br$^-$) in CF$_3$CH$_2$OH*
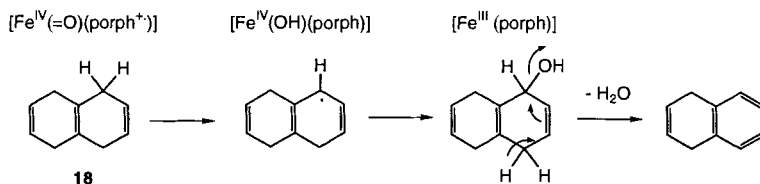
3. **Conclusions**. – With the iron(III) porphyrinate **3** and its μ-oxo dimer **4**, two cytochrome P-450 mimics were prepared that successfully model several of the properties of the natural P-450 monooxygenases.

1) In the protic solvents MeOH and CF_3CH_2OH, **3** and its metal free analog **1** form stable inclusion complexes with a variety of polycyclic aromatic hydrocarbons. The substrates are incorporated deeply into the cyclophane cavity with some C–C bonds closely approaching the porphyrin ring. The analysis of complexation-induced shifts in

the ^{1}H-NMR spectra taken from receptor-substrate complex solutions together with computer modelling indicate that acenaphthylene prefers a productive 'equatorial' inclusion geometry with the reactive 1,2-bond oriented towards the porphyrin plane (of **1**), whereas the reactive 9,10-bond of 'axially' incorporated phenanthrene is oriented away from the porphyrin ring in an unproductive binding mode.

2) In CF_3CH_2OH in the presence of iodosylbenzene as O-transfer agent, the Fe^{III} derivative **3** catalyzes the oxidation of productively bound acenaphthylene to acenaphthen-1-one (**14**). Several experiments suggest that this reaction takes place in the cyclophane cavity rather than on the open side of the porphyrin. Phenanthrene acts as a competitive inhibitor, possibly as a result of strong but unproductive binding. The μ-oxo dimer **4**, which allows substrate approach to the Fe-center only through complexation in the cyclophane cavity, shows a high catalytic activity in the oxidation of acenaphthylene in MeOH. In this solvent, the dimer is stable with regard to dissociation into two monomers. A major problem encountered in all reactions in alcoholic solvents is the poor mass balance: even in the absence of iron-porphyrinate catalyst, a large part of the initial acenaphthylene reacts, presumably together with iodosylbenzene and solvent, to give polymeric material. The nature of this unfavorable side reaction channel, which is not observed with simple iron(III) *meso*-tetraphenylporphyrinates in an aprotic solvent like CH_2Cl_2, remains unclear.

3) In an interesting mimic of cytochrome P-450 aromatase activity, isotetralin (**18**) is converted with high catalytic turnover by **3** to 1,4-dihydronaphthalene and naphthalene in CF_3CH_2OH using PhIO as O-transfer agent.

The results obtained with the μ-oxo dimer **4** strongly suggest that supramolecular catalysis is effective; however, investigations with μ-oxo dimers are limited to solvents where they do not dissociate. An enhanced versatility in the choice of reaction conditions, needed to clarify the origin of the poor mass balances in protic solvents, would be reached with a supramolecular catalyst in which cyclophane binding sites cap both sides of one porphyrin ring. Also, electron-withdrawing substituents should be introduced into the *meso*-aryl rings and at the open *meso*-positions [39] to stabilize the porphyrin moiety towards destructive self-oxidation processes. Attempts to create a supramolecular catalyst which incorporates these desirable features are now under way.

Experimental Part

General. All chemicals were reagent grade and used as received. CH_2Cl_2 was purified by distilling from CaH_2 under Ar. Tetrahydrofuran (THF) was distilled from sodium benzophenone ketyl under Ar. Acetone was dried over K_2CO_3 and filtered. Trimethyl orthoformate was dried over K_2CO_3 and distilled immediately before use. Dimethylformamide (DMF) was dried by storage over basic alumina (*E. Merck*, activity I) followed by filtration through *Celite*. Millipored H_2O was employed in ion-exchange chromatography and in all manipulations involving the quaternized ammonium compounds. Iodosylbenzene (PhIO) was prepared from iodobenzene diacetate by literature methods [40]. Acenaphthylene (85%; remainder acenaphthene) was purified by refluxing in benzene with an excess of 2,3-dichloro-5,6-dicyano-*p*-benzoquinone (DDQ). Phenanthrene was recrystallized from EtOH. Solvents for optical spectroscopy and electrochemistry were spectroanalytical grade. Chloroiron(III) tetraphenylporphyrinate [FeCl(tpp)] and $AgSbF_6$ were gifts from the group of Professor *J. S. Valentine*, UCLA. Evaporations (*in vacuo*) were carried out at water-aspirator pressure. *Anal. GC: Hewlett-Packard-5880A* gas chromatograph; 0.25 μ *DB17* capillary column (*J&W Scientific, Inc.*). *GC/MS: Hewlett-Packard-5890A* gas chromatograph with a 0.25 μ *DB17* capillary column, interfaced with a *Hewlett-Packard-5790* mass selective detector. Medium-pressure liquid chromatography (MPLC): *Perkin-Elmer-10* liquid chromatograph pump; pump pressure usually *ca.* 7 bar;

E. Merck silica gel *60* (0.04–0.063 mm). Column chromatography (CC): *E. Merck* silica gel *60* (0.04–0.063 mm and 0.063–0.200 mm). Anal. TLC: plates precoated with *E. Merck* silica gel F_{254}. M.p.: *Büchi* apparatus (Dr. *Tottoli*); uncorrected. Cyclic voltammetry: *Princeton-Applied-Research* (*PAR*) potentiostat, model *273*; data storage and manipulation with model *270* electrochemical analysis system. UV/VIS Spectra (λ_{max} (log ε)): *Varian-Cary-2300* spectrophotometer. IR Spectra (cm^{-1}): *Perkin-Elmer-1600*-FTIR or *Perkin-Elmer-520B* instrument. ^{1}H-NMR Spectra: *Bruker-AF200, -AM360,* and *-AM500* instruments; chemical shift values δ (ppm) in CDCl$_3$ rel. to internal tetramethylsilane (TMS) as standard, in other solvents, rel. to the solvent peaks ((CD$_3$)$_2$SO, *quint.* at 2.49 ppm; (D$_6$)benzene, *s* at 7.15 ppm; *p*-(D$_{10}$)xylene, *s* at 6.69 ppm); *J* in Hz; arbitrary numbering of the *meso*-aryl rings of porphyrin derivatives as well as in precursors **5–7, 9,** and **11** (see *Fig. 1*); enhancement of arom. coupling patterns by *Gaussian* multiplication of the FID's. ESR Spectra: *Bruker-ER-200D-SRC* instrument with a *4102ST* X-band rectangular cavity. MS (*m/z* (%)): *AEI-MS902* high-resolution mass spectrometer at UCLA or on *VG-ZAB2FHF* or *VG-7070EHF* instruments at UC Riverside; EI at 70 eV, FAB in a 3-nitrobenzyl alcohol matrix. Elemental analyses were done by *Spang Microanalytical Laboratory*, Eagle Harbor, MI. CAS Registry Services provided names for compounds **9, 11, 1, 3,** and **3**(3 SbF$_6^-$ instead of 3 Br$^-$). Names of other compounds were derived from these.

Complexation Studies. Samples were weighed using a *Sartorius 4503* microbalance, and all soln. preparations were done with *Eppendorf* micropipettes. ^{1}H-NMR Titrations were performed on a *Bruker-AM500* spectrometer, thermostated at 293.0 K. Samples were prepared by transferring 0.5 ml volumes of a stock soln. of the guest to preweighed samples of the host in half-dram vials. The samples were directly transferred to 0.5-mm-diameter NMR tubes. Quantitative binding numbers (K_a, ΔG°, and $\Delta \delta_{sat}$) were obtained by measuring the complexation-induced changes in chemical shift of protons of the guest and plotting these values against host concentration in a nonlinear least-squares curve-fitting routine. The reported K_a and ΔG° values are averages of those calculated from all protons of a guest that could be monitored during the titrations. UV/VIS Titrations were performed on a *Varian-Cary-2300* spectrophotometer thermostated at 293.0 K using 0.2-cm quartz cuvettes. Aliquots of a stock soln. of the guest were added to a stock soln. of the host, and solvent was added to give a final volume of 2.0 ml. Quantitative binding numbers (K_a, ΔG°, and ΔOD_{sat}) were calculated from the UV/VIS titrations by measuring the changes in optical density (*OD*) at various wavelengths and plotting these changes against the concentration of the guest using a nonlinear least-squares curve fitting routine. In the titration of **3** with phenanthrene in CF$_3$CH$_2$OH, ΔOD values were recorded at 364 and 403 nm; in the titration with the same guest and **1** in MeOH, ΔOD values were recorded at 380 nm.

Electrochemistry. All cyclic voltammetry experiments were performed in a single-compartment cell of 3-ml volume. The cell consisted of an outer water jacket which was connected to a thermostat. All experiments were performed at 20°. The working electrode was a 1 mm-diameter glassy carbon disk (*Cypress* system). Prior to each series of experiments, the electrode was polished with 0.05 μm alumina and then washed with MeOH. The reference was Ag/AgCl in MeOH (−20 mV *vs.* SCE and the potential drifted by < 5 mV in 3 h). A Pt wire served as the counter electrode. All solns. were prepared in MeOH containing 0.1M LiCl/0.06M HCl as supporting electrolyte. Acidic solns. were used to prevent the formation of the *μ*-oxo dimer. The solns. were purged with Ar prior to measurements; during measurements, a stream of Ar was passed over the solns. Ar was purified by first passing through BTS catalyst (*Fluka/BASF R3-11*) which was reduced with H$_2$ gas at 100°, then through soda lime, and finally silica gel. The purified Ar was presaturated with MeOH before use. For the investigation of the effect of substrate binding, the substrates were added in solid form into the porphyrin solns. in the cell, and the solns. were stirred until all solids dissolved.

Epoxidations. Anal. epoxidations were carried out as follows: A soln. of the porphyrin host (0.8 mM) and acenaphthylene (20 mM) was prepared in CF$_3$CH$_2$OH or MeOH. If phenanthrene was used as an inhibitor, one-half of the porphyrin-acenaphthylene soln. was transferred to a flask containing a preweighed amount of phenanthrene (20 mM). PhIO was weighed into a third flask and CF$_3$CH$_2$OH or MeOH was added to give a concentration of *ca.* 22 mM. All solns. were thoroughly purged with Ar to remove all traces of O$_2$ and were protected from light by wrapping them with aluminum foil. The PhIO soln. was then transferred to the other solns. *via* gas-tight syringe within *ca.* 5 min. Final concentrations were generally [[Fe(porphyrin)]] = 0.4 mM, [acenaphthylene] = 10 mM, [phenanthrene] = 10 mM, and [PhIO] = 11 mM. In prep. scale reactions, iodosylbenzene was added in solid form *via* a solid addition tube within *ca.* 5 min. After a designated time period, an aliquot was removed and diluted with an equal volume of a standard soln. of naphthalene. The solns. were then analyzed by GC on a 0.25-μ *DB17* capillary column (*J&W Scientific, Inc.*) running at 30 ml/min of He flow with a program raising the temp. by 10°/min from 120 to 220°.

For calculation of response factors (f) of the reactants and products, 3 separate solns. having known concentrations of acenaphthylene, acenaphthen-1-one, phenanthrene, and naphthalene were prepared and analyzed by GC under the above mentioned conditions. The ratio of the mass of each component (M_X) relative to naphthalene (M_N) was calculated, as were the areas of the corresponding GC integrals (A_X and A_N). Naphthalene was arbitrarily assigned an f value of 1.0. The other values were arrived at with the equation $f = (A_N/M_N)/(A_X/M_X)$. The following response factors were determined this way: naphthalene (retention time t_R 3.6 min, $f = 1.0$), acenaphthylene (t_R 7.1 min, $f = 0.96$), acenaphthen-1-one (t_R 10.2 min, $f = 1.17$), and phenanthrene (t_R 11.3 min, $f = 1.0$).

Acenaphthen-1-one [37] (**14**). Through a soln. of **13** (60 mg, 85 µmol) and acenaphthylene (248 mg, 1.63 mmol) in 50 ml of CH_2Cl_2 and 20 ml of CF_3CH_2OH, Ar was bubbled for 10 min. Then 500 mg (2.27 mmol) of iodosylbenzene were added portionwise *via* a solid-addition tube. After stirring overnight (the reaction was essentially over within 1 h), the soln. was shaken with aq. Na_2SO_3 soln., washed with H_2O (1 ×), dried (Na_2SO_4), and evaporated and the residue submitted to flash chromatography (FC; silica gel, CH_2Cl_2/hexanes 3:1): 158 mg (58%) of **14**. Light-brown solid. IR (KBr): 1713. ^{1}H-NMR (360 MHz, CDCl$_3$): 3.81 (*s*, H–C(2)); 7.49 (*dd*, $J = 6.9$, 1.0, H–C(3)); 7.61 (*dd*, $J = 8.4$, 6.9, H–C(4)); 7.73 (*dd*, $J = 8.1$, 7.0, H–C(7)); 7.84 (*dd*, $J = 8.4$, 1.0, H–C(5)); 7.92 (*dd*, $J = 7.0$, 0.8, H–C(8)); 8.11 (*dd*, $J = 8.1$, 0.8, H–C(6)). HR-MS: 168.0557 (C$_{12}$H$_8$O, calc. 168.0575).

2-(Trimethylsilyl)ethyl 3,4-Dimethyl-1H-pyrrole-2-carboxylate (**10**). Ethyl 3,4-dimethyl-1H-pyrrole-2-carboxylate [22] (4.30 g, 25.7 mmol) was stirred at 85–90°/*ca.* 50 Torr in the presence of 2-(trimethylsilyl)ethanol (28.4 g, 0.24 mol) and NaOMe (105 mg, 1.9 mmol). After 4.5 h, additional 35 mg (0.63 mmol) of NaOMe were added (TLC after 1 h: reaction complete). The excess of 2-(trimethylsilyl)ethanol was recovered by distillation *in vacuo* and the resulting residue partitioned between CH_2Cl_2 and H_2O. The org. layer was washed again with H_2O, dried (Na_2SO_4), and evaporated, to give a yellow oil. Upon standing, white crystalline material precipitated. The solid was dried at 10^{-5} Torr: 4.8 g (78%) of fine white solid. Material for elemental analysis was obtained by recrystallization from 2,2,4-trimethylpentane. M.p. 68–69°. IR (KBr): 3300, 1660. ^{1}H-NMR (360 MHz, CDCl$_3$): 0.06 (*s*, Me$_3$Si); 1.05–1.15 (*m*, CH$_2$Si); 2.01 (*d*, J(Me,CH) = 0.57, *Me*-pyr); 2.27 (*s*, *Me*-pyr); 4.3–4.4 (*m*, CO$_2$CH$_2$); 6.65 (*d*, J(CH,NH) = 2.6, NCH); 8.6–8.8 (br. *s*, NH). EI-MS (20 eV): 239 (M^+). Anal. calc. for C$_{12}$H$_{21}$NO$_2$Si (239.39): C 60.21, H 8.84, N 5.85; found: C 60.06, H 8.95, N 5.87.

Ethyl 4-(2-Formylphenoxy)butanoate (**5**). Salicylaldehyde (11.0 ml, 0.103 mol) was added with stirring to K$_2$CO$_3$ (34.5 g, 0.250 mol) and DMF (100 ml). The soln. was heated to 90° while being flushed with Ar. Ethyl 4-bromobutanoate (14.7 ml, 0.103 mol) in DMF (71 ml) was added dropwise over 1 h with stirring. After stirring for an additional 4 h at 90°, the mixture was filtered through *Celite* and evaporated to give an amber oil which was dissolved in AcOEt and extracted with 2N Na$_2$CO$_3$ (7 ×) and H$_2$O (1 ×). The org. phase was dried (Na$_2$SO$_4$) and evaporated: 22.7 g (93%) of a yellow liquid which was pure by ^{1}H-NMR. IR (neat): 1735, 1685. ^{1}H-NMR (360 MHz, CDCl$_3$): 1.24 (*t*, $J = 7.1$, *Me*CH$_2$O); 2.17 (*m*, CH$_2$CH$_2$CH$_2$); 2.53 (*t*, $J = 7.2$, CH$_2$CO$_2$Et); 4.13 (*t*, $J = 6.1$, ArOCH$_2$); 4.13 (*q*, $J = 7.1$, MeCH$_2$O); 6.96 (*dd*, $J(D,C) = 8.4$, $J(D,B) = 0.8$, H$_D$); 7.00 (*dddd*, $J(B,A) = 7.9$, $J(B,C) = 7.3$, $J(B,D) = 0.8$, $J(B,CHO) = 0.8$, H$_B$); 7.52 (*ddd*, $J(C,D) = 8.4$, $J(C,B) = 7.3$, $J(C,A) = 1.9$, H$_C$); 7.81 (*dd*, $J(A,B) = 7.9$, $J(A,C) = 1.9$, H$_A$); 10.48 (*d*, $J = 0.8$, CHO). EI-MS (20 eV): 236 (2, M^+), 218 (11, $[M - H_2O]^+$), 191 (9, $[M - OEt]^+$), 116 (100, $[M - C_7H_4O_2]^+$). HR-MS (EI): 236.1059 (C$_{13}$H$_{16}$O$_4$, calc. 236.1049).

4-(2-Formylphenoxy)butanoic Acid (**6**). A soln. of **5** (17.0 g, 0.072 mol) in 336 ml of MeOH and 336 ml of 2.0N KOH was heated to reflux for 90 min. Most of the MeOH was evaporated and the remaining soln. acidified to pH 1 with 3N HCl. Filtration afforded a pale yellow crystalline solid (12.81 g, 85%). M.p. 91–92.5°. IR (KBr): 3300–2400 (br.), 1709, 1685. ^{1}H-NMR (360 MHz, C$_6$D$_6$): 1.67 (*m*, CH$_2$CH$_2$CH$_2$); 2.12 (*t*, $J = 7.0$, CH$_2$CO$_2$H); 3.35 (*t*, $J = 6.1$, ArOCH$_2$); 6.31 (*dd*, $J(D,C) = 8.4$, $J(D,B) = 0.9$, H$_D$); 6.64 (*dddd*, $J(A,B) = 7.7$, $J(B,C) = 7.3$, $J(B,D) = 0.9$, $(J(B,CHO) = 0.7$, H$_B$); 7.02 (*ddd*, $J(C,D) = 8.4$, $J(C,B) = 7.3$, $J(C,A) = 1.8$, H$_C$); 7.97 (*dd*, $J(A,B) = 7.7$, $J(A,C) = 1.8$, H$_A$); 10.62 (*d*, $J = 0.7$, CHO). EI-MS (20 eV): 208 (3, M^+), 122 (100, $[M - (CH_2)_3CO_2H]^+$). Anal. calc. for C$_{11}$H$_{12}$O$_4$ (208.22): C 63.45, H 5.81; found: C 63.53, H 5.77.

Succinimido 4-(2-Formylphenoxy)butanoate (**7**). A soln. of *N,N'*-dicyclohexylcarbodiimide (10.9 g, 0.0528 mol) in 1,4-dioxane (40 ml) was added with stirring to a mixture of *N*-hydroxysuccinimide (6.08 g, 0.0528 mol) and **6** (10.0 g, 0.0408 mol) in 1,4-dioxane (100 ml). After stirring for 4 h under a drying tube (CaSO$_4$), the mixture was filtered to give a greenish-yellow soln. The solvent was removed to leave a yellow oil which solidified after drying at 10^{-1} Torr. The solid was recrystallized from CHCl$_3$/i-PrOH: 12.68 g (87%) of light brown crystals. M.p. 119–123°. IR (KBr): 1815, 1785, 1735, 1675. ^{1}H-NMR (360 MHz, CDCl$_3$): 2.31 (*m*, CH$_2$CH$_2$CH$_2$); 2.84 (*s*, COCH$_2$CH$_2$CO); 2.88 (*t*, $J = 7.1$, CH$_2$CO$_2$); 4.20 (*t*, $J = 6.1$, ArOCH$_2$); 6.99 (*dd*, $J(D,C) = 8.4$, $J(D,B) = 0.9$, H$_D$); 7.04 (*dddd*, $J(B,A) = 7.7$, $J(B,C) = 7.3$, $J(B,D) = 0.9$, $J(B,CHO) = 0.8$, H$_B$); 7.54 (*ddd*, $J(C,D) = 8.4$, $J(C,B) = 7.3$, $J(C,A) = 1.8$, H$_C$); 7.84 (*dd*, $J(A,B) = 7.7$, $J(A,C) = 1.8$, H$_A$); 10.47 (*d*, $J(CHO,B) = 0.8$, CHO). EI-MS (20 eV): 305 (M^+). Anal. calc. for C$_{15}$H$_{15}$NO$_6$ (305.29): C 59.02, H 4.95, N 4.59; found: C 58.93, H 4.87, N 4.66.

1,1″-Diethyl-10′,26′-bis[4-(2-formylphenoxy)-1-oxobutyl]-5′,15′,21′,31′,34′,35′,38′,39′-octamethyldispiro[piperidine-4,2′-[7,13,23,29]tetraoxa[10,26]diazapentacyclo[28.2.2.2³,⁶.2¹⁴,¹⁷.2¹⁹,²²]tetraconta[3,5,14,16,19,21,30,32,33,35,37,39]dodecaene-18′,4″-piperidine] (**9**). A soln. of 5.04 g (5.96 mmol) of **8** [21a] and 4.16 g (13.6 mmol) of **7** in 70 ml of 1,4-dioxane was heated to 80° for 2.5 h under Ar. After evaporation the residue was adsorbed on silica gel and submitted to FC (5 cm × 28 cm, AcOEt→AcOEt/Et₃N 95:5). The product fractions were washed with 2N Na₂CO₃ (2 ×) and H₂O (1 ×), dried (Na₂SO₄), and evaporated: 5.49 g (75%) of a white foam. Material for elemental analysis was obtained by MPLC (silica gel, AcOEt/Et₃N 95:5, 10 ml/min). IR (KBr): 1685, 1650. ¹H-NMR (360 MHz, (CD₃)₂SO, 383 K): 0.94 (*t*, *J* = 7.1, 2 *Me*CH₂); 2.07 (*s*, 24 H, arom. Me); 2.11 (*m*, 4 H, CH₂C*H₂*CH₂); 2.24 (*q*, *J* = 7.2, 4 H, CH₂CON); 2.15–2.3 (*m*, 8 H, NC*H₂*CH₂C); 2.3–2.4 (*m*, 8 H, NCH₂C*H₂*C); 2.69 (*t*, *J* = 7.1, 2 Me*CH₂*); 3.76 (*t*, *J* = 6.0, 8 H, NC*H₂*CH₂O); 3.87 (*t*, *J* = 6.0, 8 H, OC*H₂*CH₂N); 4.21 (*t*, *J* = 6.3, 4 H, OC*H₂*CH₂CH₂); 6.82 (*s*, 8 H, Me₂C₆*H₂*); 7.03 (*dddd*, *J*(B,A) = 7.7, *J*(B,C) = 7.3, *J*(B,D) = 1.1, *J*(B,CHO) = 0.7, 2 H, H_B); 7.16 (*ddd*, *J*(D,C) = 8.5, *J*(D,B) = 1.1, *J*(D,A) = 0.5, 2 H, H_D); 7.56 (*ddd*, *J*(C,D) = 8.5, *J*(C,B) = 7.3, *J*(C,A) = 1.9, 2 H, H_C); 7.65 (*ddd*, *J*(A,B) = 7.7, *J*(A,C) = 1.9, *J*(A,D) = 0.5, 2 H, H_A); 10.37 (*d*, *J*(CHO,B) = 0.7, 2 H, CHO). FAB-MS: 1225 (40, *M*⁺), 1226 (100, [*M* + 1]⁺), 1227 (76, [*M* + 2]⁺), 1228 (32, [*M* + 3]⁺). Anal. calc. for C₇₆H₉₆N₄O₁₀ (1225.63): C 74.48, H 7.89, N 4.57; found: C 74.48, H 7.92, N 4.66.

Tetrakis[2-(trimethylsilyl)ethyl] 5,5′,5″,5‴-{1,1″-Diethyl-5′,15′,21′,31′,34′,35′,38′,39′-octamethyldispiro[piperidine-4,2′-[7,13,23,29]tetraoxa[10,26]diazapentacyclo[28.2.2.2³,⁶.2¹⁴,¹⁷.2¹⁹,²²]tetraconta[3,5,14,16,19,21,30,32,33,35,37,39]dodecaene-18′,4″-piperidine]-10′,26′-diyl}bis{[(4-oxobutane-4,1-diyl)oxy]phen-2,1-ylenemethylidyne}-3,3′,3″,3‴,4,4′,4″,4‴-octamethyltetrakis(1H-pyrrole-2-carboxylate) (**11**). A soln. of 4.20 g (17.5 mmol) of **10** and 5.38 g (4.39 mmol) of **9** was heated to reflux under N₂ in 27 ml of abs. EtOH. MeSO₃H (0.60 ml, 9.2 mmol) was then added and the mixture stirred at reflux for 30 min (TLC (AcOEt/Et₃N 9:1): reaction complete). The cooled soln. was diluted with CH₂Cl₂, washed once with 2N Na₂CO₃ and with H₂O, dried (Na₂SO₄), and evaporated. The residue was separated on alumina (*Merck*, act. II–III; column 7 × 30 cm); removal of impurities with CH₂Cl₂/hexane 1:1, then slow polarity increase to AcOEt/MeOH 98:2: 7.1 g (75%) of **11**. Light yellow foam. Material for elemental analysis was obtained by MPLC (silica gel, AcOEt/Et₃N 95:5, 10 ml/min). IR (KBr): 3460, 1685, 1655. ¹H-NMR (500 MHz, (CD₃)₂SO, 393 K): 0.01 (*s*, 36 H, Me₃Si); 0.94 (*t*, *J* = 7.1, 2 *Me*CH₂); 1.03 (*m*, 8 H, CH₂Si); 1.73 (*s*, 12 H, *Me*-pyr); 1.9–2.0 (*m*, 4 H, CH₂C*H₂*CH₂); 2.07 (*s*, 24 H, *Me*₂C₆H₂); 2.18 (*s*, 12 H, *Me*-pyr); 2.2–2.3 (*m*, 12 H, >CCH₂ (pip), CH₂CON); 2.35–2.45 (*m*, 8 H, NCH₂ (pip)); 2.45 (*m*, 2 Me*CH₂*); 3.72 (*t*, *J* = 6.1, 8 H, OC*H₂*CH₂N); 3.88 (*t*, *J* = 6.1, 8 H, OCH₂C*H₂*N); 3.98 (*t*, *J* = 6.4, 4 H, OC*H₂*CH₂CH₂); 4.28 (*m*, 8 H, CH₂CH₂Si); 5.87 (*s*, 2 H, C*H*(pyr)₂); 6.82 (*s*, 8 H, Me₂C₆*H₂*); 6.89 (*ddd*, *J*(B,A) = 7.6, *J*(B,C) = 7.3, *J*(B,D) = 1.4, 2 H, H_B); 6.97 (*dd*, *J*(D,C) = 8.2, *J*(D,B) = 1.4, 2 H, H_D); 7.06 (*dd*, *J*(A,B) = 7.6, *J*(A,C) = 1.7, 2 H, H_A); 7.21 (*ddd*, *J*(C,D) = 8.2, *J*(C,B) = 7.3, *J*(C,A) = 1.7, 2 H, H_C); 9.63 (*s*, 4 H, NH). FAB-MS: 2145 (21, *M*⁺), 2146 (48, [*M* + 1]⁺), 2147 (90, [*M* + 2]⁺), 2148 (100, [*M* + 3]⁺), 2149 (78, [*M* + 4]⁺), 2150 (22, [*M* + 5]⁺). Anal. calc. for C₁₂₄H₁₇₆N₈O₁₆Si₄ (2147.17): C 69.36, H 8.26, N 5.22; found: C 69.42, H 8.34, N 5.28.

[SP-4-1]-{1,1″-Diethyl-7′,8′,11′,12′,24′,25′,29′,30′-octahydro-15′,21′,38′,39′,43′,44′,50′,51′,56′,57′,64′,68′,72′,74′,79′,82′-hexadecamethyldispiro[piperidine-4,18′-[54H-10,26](ethanoxy[1,4]benzenomethano[1,4]benzenoxyethano)[14,17:19,22]dietheno[42,45]imino[37,40]nitrilo[36,46]([2,5]-endo-pyrrolomethano[2]pyrrolyl[5]-ylidene)[10H,18H,26H,40H]dibenzo[j,w][1,9,25,33,4,30]tetraoxadiazacyclodotetracontine-69′,4″-piperidine]-9′,27′(6′H,28′H)-dionato(2-)-N⁴⁸′,N⁵⁴′,N⁵⁸′,N⁵⁹′}zinc (**2**). For 2 h, **11** (3.0 g, 1.39 mmol) was treated with 1.0M Bu₄NF/THF (11.1 ml, 11.1 mmol) in dry THF (10 ml) at 45–50° (TLC monitoring (reversed phase, MeOH/H₂O 9:1)). After evaporation, the residue was dried at 10⁻¹ Torr and the resulting dark orange foam dissolved in 700 ml of dry CH₂Cl₂ and treated with trimethyl orthoformate (4.25 ml, 3.88 mmol) and CF₃COOH (18.6 g, 114 mmol). The soln. was stirred in the dark for 4 h, while protected from moisture with a drying tube (CaSO₄). A slurry of Zn(OAc)₂·2 H₂O (730 mg, 3.33 mmol) in dry MeOH (5 ml) was then added and the mixture stirred for additional 44 h. The soln. was washed once each with 2N Na₂CO₃ and H₂O, dried (Na₂SO₄), and evaporated. This procedure was then repeated with more **11** (2.7 g). The combined residues of the two batches were heated to reflux with Zn(OAc)₂·2 H₂O (1.2 g) in CHCl₃/MeOH 1:1 (300 ml) until the VIS spectrum indicated complete metallation. The material obtained after evaporation of the solvent was adhered to silica gel and submitted to FC (AcOEt/Et₃N 95:5) under Ar. The first of the two red-fluorescent bands (*R_f* 0.30) contained **2**, the second (*R_f* 0.18) its atropisomer. The pure fractions were washed with 2N Na₂CO₃ (1 ×) and H₂O (1 ×), dried (Na₂SO₄), and evaporated: **2** as a red solid (9% yield). M.p. 248° (dec.). IR (KBr): 1650. UV/VIS (CH₂Cl₂): 575 (3.95), 539 (4.20), 502 (3.49), 411 (5.47). ¹H-NMR (500 MHz, *p*-(D₁₀)xylene, 393 K): 0.60 (br. *m*, 8 H); 1.04 (*t*, *J* = 7.1, 2 Me*CH₂*); 1.6–1.9 (*m*, 32 H); 2.26 (*q*, *J* = 7.1, 4 H, Me*CH₂*); 2.3–2.6 (*m*, 24 H); 2.75 (*s*, 12 H, *Me*-pyr); 3.56 (*s*, 12 H, *Me*-pyr); 4.08 (*t*, *J* = 6.4, 4 H, OC*H₂*CH₂CH₂); 6.75 (br. *s*, 8 H, Me₂C₆*H₂*); 7.26 (*ddd*, *J*(B,C) = 7.5, *J*(B,A) = 7.1, *J*(B,D) = 1.2, 2 H, H_B); 7.36 (*dd*, *J*(D,C) = 8.3, *J*(D,B) = 1.2, 2 H, H_D); 7.61 (*dd*, *J*(A,B) = 7.1, *J*(A,C) = 1.6, 2 H,

H_A); 7.69 (*ddd*, $J(C,D) = 8.3$, $J(C,B) = 7.5$, $J(C,A) = 1.6$, 2 H, H_C); 10.19 (*s*, 2 H, *meso*-H). FAB-MS: 1650 (100, M^+), 1651 (97, $[M + 1]^+$), 1652 (68, $[M + 2]^+$). Anal. calc. for $C_{102}H_{120}N_8O_8Zn$ (1651.52): C 74.18, H 7.32, N 6.78; found: C 74.24, H 7.38, N 6.75.

*1,1″-Diethyl-7′,8′,11′,12′,24′,25′,29′,30′-octahydro-15′,21′,38′,39′,43′,44′,50′,51′,56′,57′,64′,68′,72′,74′,79′,82′-hexadecamethyldispiro[piperidine - 4,18′ - [54*H - 10, 26*](ethanoxy[1, 4]benzenomethano[1, 4]benzenoxyethano) - [14,17:19,22]dietheno[42,45]imino[37,40]nitrilo[36,46]([2,5]* - endo - *pyrrolometheno[2]pyrrolyl[5]ylidene) - [10*H, 18*H, 26*H, 40*H]dibenzo[*j,w*]*[1, 9, 25, 33, 4, 30]tetraoxadiazacyclodotetracontine - 69′, 4″ - piperidine] - 9′,27′(6′*H,28′*H*)-dione* (1). A soln. of **2** in MeOH/conc. HCl soln. 1:1 was briefly swirled. Sat. Na_2CO_3 soln. was carefully added to neutralize the soln., followed by CH_2Cl_2. The org. layer was washed with 2N Na_2CO_3 (1 ×) and H_2O (1 ×), dried (Na_2SO_4), and evaporated: red crystalline **1** (*ca.* 100%). M.p. 225°. VIS: demetallation complete. UV/VIS (CH_2Cl_2): 628 (3.10), 576 (3.78), 541 (3.69), 507 (4.16), 409 (5.25), 277 (sh, 4.04), 271 (4.05). ^{1}H-NMR (500 MHz, *p*-(D_{10})xylene, 393 K): −1.56 (br. *s*, 2 H, NH); 0.5–0.6 (*m*, 4 H); 1.05 (*t*, $J = 7.1$, 6 H, 2 *Me*CH_2); 1.4–1.5 (*m*, 2 H); 1.55–1.65 (*m*, 10 H); 1.76 (br. *s*, 24 H, $Me_2C_6H_2$); 2.1–2.25 (*m*, 8 H); 2.28 (*q*, $J = 7.1$, 2 MeCH_2); 2.3–2.6 (*m*, 16 H); 2.77 (*s*, 12 H, *Me*-pyr); 3.54 (*s*, 12 H, *Me*-pyr); 4.04 (*t*, $J = 6.4$, 4 H, O$CH_2CH_2CH_2$); 6.76 (*s*, 8 H, $Me_2C_6H_2$); 7.23 (*ddd*, $J(B,A) = 7.5$, $J(B,C) = 7.5$, $J(B,D) = 1.2$, 2 H, H_B); 7.36 (*dd*, $J(D,C) = 8.3$, $J(D,B) = 1.2$, 2 H, H_D); 7.55 (*dd*, $J(A,B) = 7.5$, $J(A,C) = 1.6$, 2 H, H_A); 7.67 (*ddd*, $J(C,D) = 8.3$, $J(C,B) = 7.5$, $J(C,A) = 1.6$, 2 H, H_C); 10.21 (*s*, 2 H, *meso*-H). FAB-MS: 1589 (38, $[M + 2]^+$), 1588 (82, $[M + 1]^+$), 1587 (100, M^+), 795 ($M^{2+} + 1$). Anal. calc. for $C_{102}H_{122}N_8O_8$ (1588.16): C 77.14, H 7.74, N 7.06; found: C 76.87, H 7.62, N 7.11.

[SP-5-12]-Bromo-{*1,1″-Diethyl-7′,8′,11′,12′,24′,25′,29′,30′-octahydro-15′,21′,38′,39′,43′,44′,50′,51′,56′,57′,64′,68′,72′,74′,79′,82′-hexadecamethyldispiro[piperidine-4,18′-[54*H-10,26]*(ethanoxy[1,4]benzenomethano[1,4]benzenoxyethano)[14, 17:19, 22]dietheno[42, 45]imino[37, 40]nitrilo[36, 46]([2, 5]* - endo - *pyrrolometheno[2]pyrrolyl[5]ylidene)[10*H,18*H,26*H,40*H]dibenzo[*j,w*]*[1,9,25,33,4,30]tetraoxadiazacyclodotetracontine-69′,4″-piperidine]-9′,27′(6′*H,28′*H*)-dionato(2-)-N*$^{48′}$,N$^{54′}$,N$^{58′}$,N$^{59′}$}*iron Dihydrobromide* (3). Anh. $FeBr_2$ (155 mg, 0.719 mmol) was added to a soln. of **1** (167 mg, 0.105 mmol) in dry THF (25 ml), and the mixture was refluxed under Ar for *ca.* 90 min (VIS: complete reaction). The crude material was chromatographed (silica gel, CH_2Cl_2/MeOH/Et_3N 90:5:5). The combined product fractions were washed with 2N Na_2CO_3 (1 ×), H_2O (1 ×), 2% HBr soln. (1 ×), and H_2O, dried (Na_2SO_4), and evaporated. A purple/black solid (123 mg, 61%) was obtained by slow evaporation of CH_2Cl_2 from AcOEt/CH_2Cl_2. M.p. 277°. UV/VIS (CH_2Cl_2): 652 (3.45), 589 (sh, 3.40), 540 (sh, 3.81), 507 (3.94), 394 (4.97). UV/VIS (MeOH): 620 (sh, 3.42), 572 (sh, 3.47), 501 (3.83), 399 (4.87), 360 (sh, 4.42). ^{1}H-NMR (500 MHz, $CDCl_3$): −74 (br. *s*, *meso*-H); 48 (*m*, *Me*-pyr); 54 (br. *s*, *Me*-pyr). FAB-MS: 1643 ($[M - H_2Br_3]^+$). Anal. calc. for $C_{102}H_{122}Br_3FeN_8O_8 \cdot 2 H_2O$ (1919.75): C 63.82, H 6.62, N 5.84; found: C 63.79, H 6.68, N 5.69.

μ-Oxo Dimer **4**. A soln. of **3** (68 mg, $3.54 \cdot 10^{-5}$ mol) in CH_2Cl_2 (1 ml) was stirred in a heterogeneous reaction with a 10% NaOH soln. (5.0 ml). After 3 h (VIS: complete conversion), the org. layer was diluted with CH_2Cl_2, washed with H_2O (1 ×), dried (Na_2SO_4), and evaporated. Recrystallization from AcOEt/heptane yielded 42 mg (72%) of a red solid. UV/VIS (CH_2Cl_2): 592 (sh, 3.89), 566 (4.11), 400 (5.08), 359 (sh, 4.82), 320 (sh, 4.69). UV/VIS (MeOH): 598 (4.00), 576 (sh, 3.98), 486 (4.24), 404 (5.23), 359 (4.86). UV/VIS (CF_3CH_2OH): 620 (3.87), 530 (sh, 4.06), 495 (4.16), 404 (5.19), 363 (4.97).

[SP-4-1]-{*1,1″-Diethyl-7′,8′,11′,12′,24′,25′,29′,30′-octahydro-15′,21′,38′,39′,43′,44′,50′,51′,56′,57′,64′,68′,72′,74′,79′,82′-hexadecamethyldispiro[piperidine-4,18′-[54*H,10,26]*(ethanoxy[1,4]benzenomethano[1,4]benzenoxyethano)[14,17:19,22]dietheno[42,45]imino[37,40]nitrilo[36,46]([2,5]*-endo-*pyrrolometheno[2]pyrrolyl[5]ylidene)[10*H,18*H,26*H,40*H]dibenzo[*j,w*]*[1,9,25,33,4,30]tetraoxadiazacyclodotetracontine-69′,4″-piperidine]-9′,27′(6′*H,28′*H*)-dionato(2-)-N*$^{48′}$,N$^{54′}$,N$^{58′}$,N$^{59′}$}{*[OC-6-11]-hexafluoroantimonato*}(*1-*)*iron Bis*{*[OC-6-11]-hexafluoroantimonate(1 −)*} (**3** (3 SbF_6^- instead of 3 Br$^-$)). A soln. of **3** (52 mg, $2.69 \cdot 10^{-5}$ mol) and $AgSbF_6$ (30 mg, $8.7 \cdot 10^{-5}$ mol; extremely hygroscopic!) in dry THF (13 ml) was stirred at r.t. under Ar for 2 h. The soln. was filtered to remove precipitated AgBr and the volume reduced on the rotary evaporator. Heptane (*ca.* 5 ml) was added and the soln. was refrigerated. A red powder (45 mg, 73%) was recovered by vacuum filtration. UV/VIS (MeOH): 610 (3.38), 577 (3.40), 501 (3.85), 399 (5.09).

REFERENCES
[1] Part VII: I. Chao, F. Diederich, *Recl. Trav. Chim. Pays-Bas* **1993**, *112*, 335.
[2] B. Morgan, D. Dolphin, *Struct. Bonding (Berlin)* **1987**, *64*, 115; J. E. Baldwin, P. Perlmutter, *Topics Curr. Chem.* **1984**, *121*, 181; B. Garcia, C.-H. Lee, A. Blaskó, T. C. Bruice, *J. Am. Chem. Soc.* **1991**, *113*, 8118; J. A. Wytko, E. Graf, J. Weiss, *J. Org. Chem.* **1992**, *57*, 1015.
[3] T. G. Traylor, *Acc. Chem. Res.* **1981**, *14*, 102; M. Momenteau, *Pure Appl. Chem.* **1986**, *58*, 1493.
[4] J. P. Collman, F. C. Anson, C. E. Barnes, C. S. Bencosme, T. Geiger, E. R. Evitt, R. P. Kreh, K. Meier, R. B. Pettman, *J. Am. Chem. Soc.* **1983**, *105*, 2694.
[5] H. Heitele, F. Pöllinger, K. Kremer, M. E. Michel-Beyerle, M. Futscher, G. Voit, J. Weiser, H. A. Staab, *Chem. Phys. Lett.* **1992**, *188*, 270; W. Frey, R. Klann, F. Laermer, T. Elsaesser, E. Baumann, M. Futscher, H. A. Staab, *ibid.* **1992**, *190*, 567; J. S. Lindsey, J. K. Delaney, D. C. Mauzerall, H. Linschitz, *J. Am. Chem. Soc.* **1988**, *110*, 3610.
[6] M. F. Powell, E. F. Pai, T. C. Bruice, *J. Am. Chem. Soc.* **1984**, *106*, 3277; D. Mansuy, *Pure Appl. Chem.* **1987**, *59*, 759; J. P. Collman, J. I. Brauman, J. P. Fitzgerald, P. D. Hampton, Y. Naruta, T. Michida, *Bull. Chem. Soc. Jpn.* **1988**, *61*, 47.
[7] Ed. P. R. Ortiz de Montellano, 'Cytochrome P-450', Plenum Press, New York, 1986; F. P. Guengerich, T. L. MacDonald, *Acc. Chem. Res.* **1984**, *17*, 9; S. D. Black, M. J. Coon, *Adv. Enzymol. Relat. Areas Mol. Biol.* **1987**, *60*, 35; J. H. Dawson, *Science (Washington, D. C.)* **1988**, *240*, 433.
[8] D. W. Nebert, F. J. Gonzalez, *Hospital Practice* **1987**, 63.
[9] C. Heidelberger, *Annu. Rev. Biochem.* **1975**, *44*, 79; R. G. Harvey, N. E. Geacintov, *Acc. Chem. Res.* **1988**, *21*, 66.
[10] T. L. Poulos, B. C. Finzel, I. C. Gunsalus, G. C. Wagner, J. Kraut, *J. Biol. Chem.* **1985**, *260*, 16122; T. L. Poulos, B. C. Finzel, A. J. Howard, *Biochemistry* **1986**, *25*, 5314; T. L. Poulos, B. C. Finzel, A. J. Howard, *J. Mol. Biol.* **1987**, *195*, 687; R. Raag, T. L. Poulos, *Biochemistry* **1989**, *28*, 917.
[11] S. Sligar, *Biochemistry* **1976**, *15*, 5399; S. G. Sligar, I. C. Gunsalus, *Proc. Natl. Acad. Sci. U.S.A.* **1976**, *73*, 1078.
[12] B. Stäubli, H. Fretz, U. Piantini, W.-D. Woggon, *Helv. Chim. Acta* **1987**, *70*, 1173; J. P. Collman, S. E. Groh, *J. Am. Chem. Soc.* **1982**, *104*, 1391; A. R. Battersby, W. Howson, A. D. Hamilton, *J. Chem. Soc., Chem. Commun.* **1982**, 1266; M. J. Gunter, P. Turner, *J. Mol. Catal.* **1991**, *66*, 121.
[13] M. J. Gunter, P. Turner, *Coord. Chem. Rev.* **1991**, *108*, 115; D. Ostovic, T. C. Bruice, *Acc. Chem. Res.* **1992**, *25*, 314; J. T. Groves, *J. Chem. Educ.* **1985**, *62*, 928; J. P. Collman, T. Kodadek, J. I. Brauman, *J. Am. Chem. Soc.* **1986**, *108*, 2588; T. G. Traylor, *Pure Appl. Chem.* **1991**, *63*, 265.
[14] J. T. Groves, P. Viski, *J. Org. Chem.* **1990**, *55*, 3628; K. Konishi, K. Oda, K. Nishida, T. Aida, S. Inoue, *J. Am. Chem. Soc.* **1992**, *114*, 1313; J. P. Collman, X. Zhang, V. J. Lee, J. I. Brauman, *J. Chem. Soc., Chem. Commun.* **1992**, 1647; S. O'Malley, T. Kodadek, *J. Am. Chem. Soc.* **1989**, *111*, 9116.
[15] J. T. Groves, T. E. Nemo, R. S. Myers, *J. Am. Chem. Soc.* **1979**, *101*, 1032.
[16] a) C. K. Chang, M.-S. Kuo, *J. Am. Chem. Soc.* **1979**, *101*, 3413; b) C. K. Chang, F. Ebina, *J. Chem. Soc., Chem. Commun.* **1981**, 778; c) J. R. Lindsay Smith, P. R. Sleath, *J. Chem. Soc., Perkin Trans. 2* **1982**, 1009; d) I. Tabushi, K. Morimitsu, *Tetrahedron Lett.* **1986**, *27*, 51; e) R. P. Hanzlik, K.-H. J. Ling, *J. Org. Chem.* **1990**, *55*, 3992.
[17] F. Diederich, *Angew. Chem.* **1988**, *100*, 372; *ibid. Int. Ed.* **1988**, *27*, 362; F. Diederich, 'Cyclophanes', The Royal Society of Chemistry, Cambridge, 1991.
[18] Preliminary communication of this work: D. R. Benson, R. Valentekovich, F. Diederich, *Angew. Chem.* **1990**, *102*, 213; *ibid. Int. Ed.* **1990**, *29*, 191.
[19] N. Kobayashi, U. Akiba, K. Takatori, A. Ueno, T. Osa, *Heterocycles* **1982**, *19*, 2011; M. C. Gonzalez, A. R. McIntosh, J. R. Bolton, A. C. Weedon, *J. Chem. Soc., Chem. Commun.* **1984**, 1138; A. Hamilton, J.-M. Lehn, J. L. Sessler, *J. Am. Chem. Soc.* **1986**, *108*, 5158; Y. Aoyama, A. Yamagishi, M. Asagawa, H. Toi, H. Ogoshi, *ibid.* **1988**, *110*, 4076; J. R. Lindsey, P. C. Kearney, R. J. Duff, T. Tjivikua, J. Rebek, Jr., *ibid.* **1988**, *110*, 6575; R. Breslow, A. B. Brown, R. D. McCollough, P. W. White, *ibid.* **1989**, *111*, 4517; Y. Aoyama, T. Motomura, H. Ogoshi, *Angew. Chem.* **1989**, *101*, 922; *ibid Int. Ed.* **1989**, *28*, 921; Y. Kuroda, T. Hiroshige, T. Sera, Y. Shoroiwa, H. Tanaka, H. Ogoshi, *J. Am. Chem. Soc.* **1989**, *111*, 1912; T. Sasaki, E. T. Kaiser, *ibid.* **1989**, *111*, 380; J. T. Groves, R. Neumann, *ibid.* **1989**, *111*, 2900; K. Eshima, Y. Matsushita, E. Hasegawa, H. Nishide, E. Tsuchida, *Chem. Lett.* **1989**, 381; I. O. Sutherland, *Pure Appl. Chem.* **1989**, *61*, 1547; R. P. Bonar-Law, J. K. M. Sanders, *J. Chem. Soc., Chem. Commun.* **1991**, 574; G. Slobodkin, E. Fan, A. D. Hamilton, *New J. Chem.* **1992**, *16*, 643; S. Anderson, H. L. Anderson, J. K. M. Saunders, *Angew. Chem.* **1992**, *104*, 921; *ibid. Int. Ed.* **1992**, *31*, 907; R. P. Bonar-Law, L. G. Mackay,

J. K. M. Sanders, *J. Chem. Soc., Chem. Commun.* **1993**, 456; C. J. Walter, H. L. Anderson, J. K. M. Sanders, *ibid.* **1993**, 458.

[20] J. E. Baldwin, M. J. Crossley, T. Klose, E. A. O'Rear (III), M. K. Peters, *Tetrahedron* **1982**, *38*, 27; G. P. Arsenault, E. Bullock, S. F. MacDonald, *J. Am. Chem. Soc.* **1960**, *82*, 4384.

[21] a) F. Diederich, K. Dick, D. Griebel, *J. Am. Chem. Soc.* **1986**, *108*, 2273; b) D. B. Smithrud, F. Diederich, *ibid.* **1990**, *112*, 339.

[22] G. M. Badger, R. A. Jones, R. L. Laslett, *Aust. J. Chem.* **1964**, *17*, 1157.

[23] H. Gerlach, *Helv. Chim. Acta* **1977**, *60*, 3039.

[24] H. M. Goff, in 'Iron Porphyrins', Eds. A. B. P. Lever and H. B. Gray, Addison-Wesley, 1983, Part I, Chapt. 4, p. 237, and ref. cit. therein; G. N. La Mar, F. A. Walker (Jensen), in 'The Porphyrins', Ed. D. Dolphin, Academic Press, New York, 1979, Vol. IV, Chapt. 2, p. 61.

[25] M. Nappa, J. S. Valentine, *J. Am. Chem. Soc.* **1978**, *100*, 5075; M. Gouterman, in 'The Porphyrins', Ed. D. Dolphin, Academic Press, New York, 1978, Vol. III, Chapt. 1, p. 1; E. B. Fleischer, J. M. Palmer, T. S. Srivastava, A. Chatterjee, *J. Am. Chem. Soc.* **1971**, *93*, 3162.

[26] D. R. Benson, R. Valentekovich, C. B. Knobler, F. Diederich, *Tetrahedron* **1991**, *47*, 2401.

[27] W. C. Still, 'Macromodel, Version 2.6', Columbia University, New York.

[28] C. Gueutin, D. Lexa, M. Momenteau, J.-M. Savéant, F. Xu, *Inorg. Chem.* **1986**, *25*, 4294; P. O'Brien, D. A. Sweigart, *ibid.* **1985**, *24*, 1405, and ref. cit. therein.

[29] R. Tsai, C. A. Yu, I. C. Gunsalus, J. Peisach, W. Blumberg, W. H. Orme-Johnson, H. Beinert, *Proc. Natl. Acad. Sci. U.S.A.* **1970**, *66*, 1157.

[30] M. T. Fisher, S. G. Sligar, *J. Am. Chem. Soc.* **1985**, *107*, 5018.

[31] C. E. Strouse, University of California, Los Angeles, unpublished results.

[32] E. Heilbronner, P. A. Straub, 'Hückel Molecular Orbitals', Springer, Berlin, 1966.

[33] T. G. Traylor, University of California, San Diego, personal communication.

[34] B. C. Schardt, C. L. Hill, *Inorg. Chem.* **1983**, *22*, 1563.

[35] T. G. Traylor, J. C. Marsters, Jr., T. Nakano, B. E. Dunlap, *J. Am. Chem. Soc.* **1985**, *107*, 5537.

[36] J. R. Lindsay Smith, D. N. Mortimer, *J. Chem. Soc., Chem. Commun.* **1985**, 410.

[37] L. F. Fieser, J. Cason, *J. Am. Chem. Soc.* **1940**, *62*, 432; A. Bosch, R. K. Brown, *Can. J. Chem.* **1968**, *46*, 715.

[38] V. F. Anikin, T. I. Levandovskaya, *Zh. Org. Khim.* **1984**, *20*, 1929; S. Krishnan, D. G. Kuhn, G. A. Hamilton, *J. Am. Chem. Soc.* **1977**, *99*, 8121; M. Imuta, H. Ziffer, *J. Org. Chem.* **1979**, *44*, 1351.

[39] J. F. Bartoli, O. Brigaud, P. Battioni, D. Mansuy, *J. Chem. Soc., Chem. Commun.* **1991**, 440; T. G. Traylor, S. Tsuchiya, *Inorg. Chem.* **1987**, *26*, 1338; P. S. Traylor, D. Dolphin, T. G. Traylor, *J. Chem. Soc., Chem. Commun.* **1984**, 279; M. J. Nappa, C. A. Tolman, *Inorg. Chem.* **1985**, *24*, 4711.

[40] H. Saltzman, J. G. Sharefkin, *Org. Syn. Coll. Vol. V* **1973**, 658.